AUTOMATED MEASUREMENTS OF DIELECTRIC ROD ANTENNA RADIATION CHARACTERISTICS

By

MAJOR RAJENDER KUMAR SHARMA

DEPARTMENT OF ELECTRICAL ENGINEERING
INDIAN INSTITUTE OF TECHNOLOGY, KANPUR

FEBRUARY, 1985

AUTOMATED MEASUREMENTS OF DIELECTRIC ROD ANTENNA RADIATION CHARACTERISTICS

A Thesis Submitted
In Partial Fulfilment of the Requirements
for the Degree of
MASTER OF TECHNOLOGY
IN
ELECTRICAL ENGINEERING

By
MAJOR RAJENDER KUMAR SHARMA

to the

DEPARTMENT OF ELECTRICAL ENGINEERING
INDIAN INSTITUTE OF TECHNOLOGY KANPUR
FEBRUARY, 1985

ACKNOWLEDGEMENT

I wish to express my gratitude and indebtedness to Dr. C. Das Gupta for his exemplary guidance and encouragement at each stage of this thesis.

It needs a special word of thanks to Prof. S.S. Prabhu, Head of the Department for his active help in designing the 'Automatic Radiation Plotter' for which he took keen interest.

Thanks are also due to Mr. S.S. Bhatnagar and Mr. S.P. Chakravorty for their timely help in the matter of constructing the plotter.

The excellent typing of Mr. J.S. Rawat has helped in bringing this thesis to its present form.

- Maj. R.K. Sharma

CERTIFICATE

Certified that the thesis entitled 'AUTOMATED MEASUREMENTS OF DIELECTRIC ROD ANTENNA RADIATION CHARACTERISTICS' by Major R.K. Sharma, has been carried out under my supervision and the same has not been submitted elsewhere for a degree.

Feb. 7 ,1985

(Dr. C. Das Gupta)
Assistant Professor
Department of Electrical Engineering
Indian Institute of Technology
Kanpur

ABSTRACT

There are very large number of antennas in the frequency bands starting from millimeter wave band down to HF range. Because of associated smaller wavelength there are already large number of antennas in millimeter and microwave frequency band with relatively small dimension and high directivity.

It becomes increasingly difficult to realise small sized antenna in the lower radio frequency range. In particular, the state of art in ELF range is very much in the pessimistic form.

Dielectric antennas had been tried during forties and fifties In our present work, we had planned our investigation with a hope to realize the dielectric antenna with suitable materials that may make some break through in this dark region. To start with and to understand the problem, standard low ϵ' Teflon samples were taken to study their radiating properties at scaled up microwave frequency range.

While carrying out measurements, difficulties were faced due to generator output instability and irregular behaviour of the test equipment/instruments. Thus, to solve this problem, an automated radiation plotter has been designed and constructed as a major part of this project work.

Subsequently, different dielectric rod antennas of Teflon material with different methods of excitation have been studied successfully in qualitative manner.

TABLE OF CONTENTS

CHAPTER 1

INTRODUCTION

1.1 GENERAL:

The study of microwave antennas had advanced on such extensive lines during the end of thirties and forties that it had been established as a separate subject within the broad field of microwave techniques. During world war II, a great need was felt for microwave antennas specially for radar applications. Many text books have been written on individual type of antennas. One of these, which has not fully developed, is Dielectric group of antennas, which is the subject of this work.

There exists a family of dielectric antennas, the principal members being -

a) The solid dielectric rod antennas
b) The hollow dielectric tube antennas
c) The dielectric horn, which is similar to the metal electromagnetic horn with the metal walls replaced by dielectric walls.

From the above three kinds of dielectric antennas which more or less offer a similar kind of study, the subject of this work is basically 'The solid dielectric rod antennas'.

1.2 HISTORICAL BACKGROUND:

Electromagnetic waves may be guided along the axis of a cylinder, of arbitrary cross-section and length, at the surface of which exists a discontinuity in the dielectric properties of the media inside and outside the cylinder. A rod of dielectric material is an example of such a system. The propagation in this kind of waveguide differs in many respects from propagation in hollow metal tubes. The major difference being that in metal tube, the electric and magnetic fields are contained within the metal whereas in the case of dielectric rod, the fields exist outside also.

1.2.1 Initial Work (1910-1938):

At first, the propagation of electromagnetic waves along a solid dielectric cylinder (rod), was investigated theoretically by HONDROS and DEBYE [1] whose work was published in 1910. Some experimental work on guided transmission in the dielectric rod was carried out by ZAHN [2] in 1916 and later the experimental work of SCHRIEVER [3] provided further confirmation of the initial theory. Later, in 1936, when experimental work at shorter wavelengths was possible, the subject was advanced by BARROW [4]; SOUTHWORTH [5] described experiments dealing with α attenuation in dielectric guides and an analysis of waveguide transmission, including the effects

of imperfect dielectrics on transmission loss was given by CARSON, MEAD and SCHELKUNOFF [6].

1.2.2 Advent of Dielectric Rod Antennas (1938-1951):

In 1938 MALLACH [7] utilised the fact that since the field is also outside the dielectric guide and the losses occur in the transmission of electromagnetic energy, the rod of dielectric excited at one end turned out to be directional radiator and hence this was the beginning of dielectric rod antennas. When correctly dimensioned, this radiator gave a single lobe radiation pattern with its maximum in the direction of the axis of the rod and its directivity proportional to the length of the rod.

Following this work, WEGENER [8] carried out a theoretical analysis of propagation along a dielectric rod in which he investigated the characteristics of symmetrical and asymmetrical modes, and the problem of attenuation. Early work by SOUTHWORTH [9] in 1940 on the radiation from dielectric rods was the beginning of the study of the subject in America, followed by work by MUELLER and TYRELL [10] commenced in 1941 and published in 1947, which consisted of an extensive experimental investigation of dielectric rod antennas and gave a method of deriving an expression for the radiation pattern. Another investigation carried out in England by

HALLIDAY and KIELY [11] in 1947 gave similar experimental and theoretical results. In 1948, a more rigid analysis of the mechanism of radiation from dielectric rods was presented by WATSON and HORTON [12] and brought the theory of the subject of radiation from dielectric rod to some advanced stage. Other contributions were also published in 1948 by SIMON [13] and WILKIES [14]. In 1950, in a paper by HORTON, KARAL and KCKINNEY [15], the theory presented by WATSON and HORTON has been applied with considerable success to the radiation of circular section dielectric rod excited in the traverse magnetic mode with radial symmetry (E_{01}). This problem is simple mathematically than that of the rod excited in the normal asymmetric hybrid mode, but the radiation pattern has a null in the forward direction so that the results though very important academically, may not be applied to practical design problems. A study of the side lobe structure of the radiation patterns of dielectric rods was presented in 1951 by WATSON [16] as a continuation of his earlier work. This added considerably to the existing information on the fine structure of these patterns.

1.2.3 Activities in the Field of Dielectric Rod Antenna (1951-1985):

Activities in the field of dielectric rod antenna in the chronological order after 1951 can be summarised in the following way.

RB ADLER [17] studied the properties of EM waves in non-homogeneous cylinderical structure. This work is in general of analytical nature. Subsequently J. BROWN and J.O. SPECTOR [18] studied the radiating properties of the dielectric rod antenna in the form of End Fire array so as to enhance the directivity of the structure. In our present work when we get better understanding of a proposed structure to be used at lower frequency, the same conventional method of End Fire structure can be incorporated to enhance its directivity. DUNCAN and DUHAMEL [19] devised technique for controlling radiation pattern of dielectric rod antenna in 1957. During 1959 ANGULU [20] derived an expression for terminal impedance for semi-infinite dielectric rod antenna by means of variational method and in this paper he had furnished the experimental results. Excitation of dipole mode [21] in dielectric rod antenna with the help of non-uniform magnetic ring was studied in 1962. A work on surface mode coupling [22] along a tapered dielectric rod confirmed that directivity increases if the rod is tapered. Characteristics of large diameter [23] dielectric rod End Fire antenna were studied in 1966. J.R. JAMES [24] carried out theoretical investigation of cylindrical dielectric rod antenna.

In 1972 Hybrid Model [25] analysis of circular semi-infinite dielectric rod antenna excited in HE_{11} hybrid mode was carried out. Also launching efficiency of HE_{11} surface wave mode was determined in 1973 [26]. Almost at the same time paper on radiation properties of a composite dielectric rod antenna was published in Electronic Letter [27]. For the first time scattering theory approach [28], was applied for calculation of antenna radiation pattern of dielectric rod antennas for TM_{01} mode in 1975.

This collected work from many sources has provided a considerable increase to the knowledge of dielectric rod antennas and brought the subject to some reasonable position, at which it stands even today.

From the literature survey it appears that though the dielectric rod antenna are finding major interest in millimeter wave region but the information, as regards their applications in the microwave and lower frequency bands during the last decade, is missing.

From intuition (which plays dominant part in the field of antenna analysis) it can be expected that dielectric rod antenna with ultra high ε' may be operative at lower microwave frequency ranges and even at lower frequencies. This in turn will facilitate a reduced size of antenna at these

frequencies. This sort of antenna will then find major applications in Satellite Communication Systems, Surveillance units and mobile communications systems.

1.3 AIM OF THE PROJECT:

The main objective of our investigations of dielectric rod antenna is to use them at lower radio frequencies (e.g.. ELF, LF, HF, VHF, UHF etc.) bands. Teflon ($\epsilon = 2.1$) rod has been used as a sample antenna in the form of receiving antenna at microwave frequency band. (The characteristics of transmitting antenna are same due to reciprocal nature of antennas). After systematic study of these Teflon antennas at Microwave frequency band, suitable dielectric materials can be substituted to be used as antenna at lower frequencies.

However, during above investigation, a great deal of difficulty was experienced while carrying out the investigations (i.e. Radiation characteristics) manually due to various reasons e.g. generator instability and behaviour of other equipments/instruments when handled manually. To overcome the above difficulties and to get reliable experimental results, it was proposed to study these dielectric rod antenna radiation characteristics at Microwave frequencies with the help of 'Automated Radiation Plotter'.

The main part of this work constitutes of design and construction of 'Automatic Radiation Plotter' and automated measurement of radiation fields of the dielectric rod antenna at scaled up Microwave frequency band.

CHAPTER 2

WAVE PROPAGATION ALONG A DIELECTRIC ROD

2.1 GENERAL:

In order to understand the radiating modes in the dielectric antenna, it is necessary to analyse the behaviour of the different modes in the dielectric sample by solving the Maxwell's equations. In this chapter we will consider most of the principal characteristics of guided wave propagation in the dielectric rod. The dependence of the wave on rod diameter and dielectric constant for the symmetric and asymmetric modes will be derived theoretically and those features of wave propagation along a rod which have a bearing on the design of dielectric rod aerials will be pointed out. The following method of analysis follows the lines indicated by WEGENER[8]. In this analysis M.K.S. units will be used.

2.1.1 Solution of Maxwell Equations:

Consider a cylinder of dielectric constant ϵ_1, and magnetic permeability μ_1, embedded in a dielectric medium of dielectric constant ϵ_2 and magnetic permeability μ_2. Conductivity in both the media is zero. The cylindrical co-ordinate system is shown in Fig. 2.1, where the co-ordinates of a point P in cylinder are $(\rho \phi Z)$.

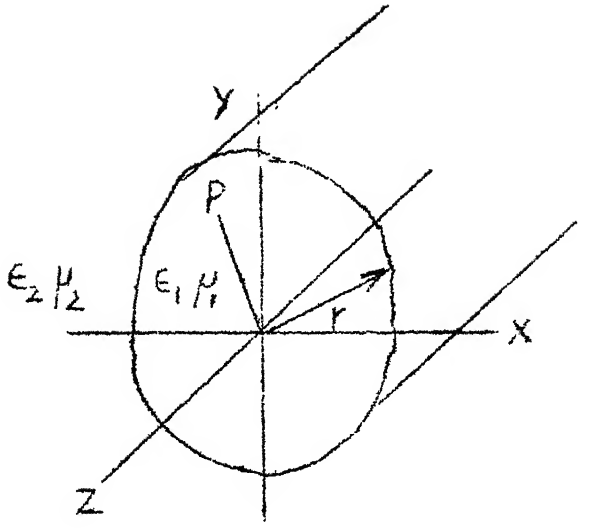

General Maxwell's equations are -

for charge free media with zero conductivity:

$$\text{Curl } E = - j\omega\mu H \qquad (2.1)$$

$$\text{Curl } H = j\omega\epsilon E \qquad (2.2)$$

and also Div E = 0 and Div H = 0

A time dependence of $e^{j\omega t}$ is assumed.

Introducing the magnetic vector potential A^H defined as $H = \text{curl } A^H$, we obtain from (2.1)

$$\text{curl } (E + j\omega\mu A^H) = 0$$

As the field of the vector $(E+j\omega\mu A^H)$ is irrotational it may therefore be derived from a scalar potential i.e.

$$E + j\omega\mu A^H = -\text{grad } \phi \ ;$$

or

$$E = -\text{grad}\ \underline{\phi} - j\omega\mu A^H \qquad (2.3)$$

From (2.2)

$$\text{curl}\ \ \text{curl}\ A^H = j\omega\epsilon E$$

$$\text{grad div}\ A^H - \nabla A^H = j\omega\epsilon E$$

$$\text{So}\ E = \frac{1}{j\omega\epsilon}\ (\text{grad div}\ A^H - \nabla A^H) \qquad (2.4)$$

By comparing (2.3) and (2.4) we see that

$$-\underline{\phi} = \frac{1}{j\omega\epsilon}\ \text{div}\ A^H$$

and we obtain the wave equation

$$A^H = -\omega^2\mu\epsilon A^H \qquad (2.5)$$

Assuming now that the magnetic vector-potential has only one component, in the direction of propagation (along the Z axis), the following set of equations for the field components are obtainted

$$E_\rho = \frac{1}{j\omega\epsilon}\left(\frac{\partial^2 A_z^H}{\partial p \partial z}\right)$$

$$E_\phi = \frac{1}{j\omega\epsilon}\left(\frac{\partial^2 A_z^H}{\partial \phi \partial z}\right)$$

$$E_z = \frac{1}{j\omega\epsilon}\left(\frac{\partial^2 A_z^H}{\partial z^2} + \omega^2\mu\epsilon\, A_z^H\right)$$

$$H_\rho = \frac{1}{\rho} \frac{\partial A_z^H}{\partial \phi}$$

$$H_\phi = - \frac{\partial A_z^H}{\partial \rho}$$

$$H_z = 0 \qquad (2.6)$$

These field equations represent an E type wave in the usual nomendature. Similarly, by introducing the electric vector potential A^E defined as

$$E = \text{curl } A^E$$

the field equations of an H type wave may be obtained. These are

$$E_\rho = \frac{1}{\rho} \frac{\partial A_z^E}{\partial \phi}$$

$$E_\phi = - \frac{\partial A_z^E}{\partial \rho}$$

$$E_z = 0$$

$$H_\rho = - \frac{1}{j\omega\mu} \left(\frac{\partial^2 A_z^E}{\partial \rho \partial z} \right)$$

$$H_\phi = - \frac{1}{j\omega\mu} \left(\frac{1}{\rho} \frac{\partial^2 A_z^E}{\partial \phi \partial z} \right)$$

$$H_z = - \frac{1}{j\omega\mu} \left(\frac{\partial^2 A_z^E}{\partial z^2} + \omega^2 \mu \epsilon A_z^E \right) \qquad (2.7)$$

2.1.2 Mode Nomenclature:

In the following analyses, wave modes in a circular section dielectric cylinder will be, in general, identified in the form H_{mn} or E_{mn} for H and E type waves respectively where m is the order of the Bessel, Neumann or Hankel functions involved in the transcendental equations to be solved for determining propagation constant and n is the root (first, second, third etc.) of equation considered.

2.2 CIRCULARLY-SYMMETRICAL FIELD DISTRIBUTION:

2.2.1 Case 1 H_o Waves:

Excitation of a wave having circularly-symmetric field components in a dielectric rod of circular section may be obtained from similar mode in metal tube guide. This mode may be represented mathematically in terms of an electric vector-potential with only one component which lies in the direction of propagation (z-direction) and from symmetry, is independent of ϕ. It is given by

$$A^E = A_z^E (\rho)\, e^{-\gamma z}$$

the time factor for harmonic oscillation $e^{j\omega t}$ being omitted here and in all subsequent field equations.

With this substitution we have the wave equation:

$\nabla A^E + \omega^2 \mu\epsilon A^E = 0$ gives the general solution as

$$A^E = [B^E J_o(k\rho) + C^E Y_o(k\rho)]e^{-\gamma z}$$

where

$$k^2 = \omega^2 \mu\epsilon + \gamma^2$$

and γ is the propagation constant of the mode.

As vector potential must be finite on the axis of the cylinder, C^E must be made zero within the cylinder as the Neumann function $Y_o(k\rho)$ tends to infinity as its argument tends to zero. So for the region within dielectric cylinder

$$A_1^E = B^E J_o(k_1\rho) e^{-\gamma_1 z}$$

where subscript 1 refers to conditions within dielectric cylinder. Outside the cylinder the Neumann function remains finite for all values of $\rho > r$ and we have

$$A_2^E = [D^E J_o(k_2\rho) + E^E Y_o(k_2\rho)] e^{-\gamma_2 z} \qquad (2.8)$$

where the subscript 2 refers to the conditions outside the dielectric cylinder.

It is convenient to replace the Bessel and Neumann functions by Hankel functions of the first and second kinds in (2.8) since these functions behave like exponential functions when their arguments are imaginary. The coefficients

D^E and E^E being as yet undetermined we may write

$$A_2{}^E = [D^E H_o{}^1(k_2\rho) + E^E H_o{}^2(k_2\rho)]e^{-\gamma_2 z}$$

To describe a non-radiating mode, that is one in which energy flows only in z direction and there is no radiation of energy radially, the argument of Hankel functions must be complex. That is, k_2 must be complex or pure imaginary and if imaginary part of it is assumed to be positive, E^E must be made zero as $H_o{}^2(k_2\rho)$ does not tend to zero as the argument increases. If, on the other hand, the imaginary part k_2 is assumed to be negative D^E must be made zero as $H_o{}^1(k_2\rho)$ does not tend to zero as the argument increases. We will assume that the former is the case (i.e. imaginary part of k_2 is made positive) and put $E^E = 0$, thus giving

$$A_2{}^E = D^E H_o{}^1 (k_2\rho)e^{-\gamma_2 z} \qquad (2.9)$$

Henceforth we shall write H_o for $H_o{}^1$

Therefore using the above equations and the field equations for H_o mode are obtained

$$E_\phi = - B^E k_1 J_o (k_1\rho)e^{-\gamma_1 z}$$

$$H_\rho = B^E \frac{\gamma_1 k_1}{j\omega\mu_1} J_o' (k_1\rho) e^{-\gamma_1 z} \qquad \text{for } \rho < r$$

$$H_z = -B^E \frac{k_1{}^2}{j\omega\mu_1} J_o(k_1\rho) e^{-\gamma_1 z}$$

and

$$E_{\phi} = - D^{E} k_2 H_o' (k_2\rho) e^{-\gamma_2 z}$$

$$H_{\rho} = D^{E} \frac{\gamma_2 k_2}{j\omega\mu_2} H_o' (k_2\rho) e^{-\gamma_2 z} \qquad \text{for } \rho > r$$

$$H_z = -D^{E} \frac{k_2^2}{j\omega\mu_2} H_o(k_2\rho) e^{-\gamma_2 z}$$

The boundary conditions at the surface $\rho = r$ require contunity of E_{ϕ}, H_z and μH_{ρ} from which follow the determining equations for the unknown $k_1, k_2, \gamma_1, \gamma_2$ and D/B

putting $x_1 = k_1 r$ and $x_2 = k_2 r$

the characteristics equation for H_o wave is, therefore

$$x_1 \frac{J_o(x_1)}{J_o'(x_1)} = \frac{\mu_1}{\mu_2} x_2 \frac{H_o(x_2)}{H_o'(x_2)} \qquad (2.10)$$

we also have by putting

$$\frac{\mu_1}{\mu_o} = \frac{\mu_2}{\mu_o} = \frac{\epsilon_2}{\epsilon_o} = 1$$

where μ_o and ϵ_o are the constants of a vaccum

$$k_1^2 - k_2^2 = (\frac{2\pi}{\lambda_1})^2 - (\frac{2\pi}{\lambda_2})^2 = (\frac{2\pi}{\lambda_o})^2 (\frac{\epsilon}{\epsilon_o} - 1)$$

As $x = k\rho$ and writing $\bar{\epsilon} = \epsilon/\epsilon_o$

$$x_1^2 - x_2^2 = (x_1)^2 + \left(\frac{x_2}{i}\right)^2 = \left(\frac{\pi d}{\lambda_o}\right)^2 (\epsilon - 1) = R^2 \qquad (2.11)$$

In solving the eqns. (2.10) and (2.11), loss free media will be assumed, there shall be no dielectric loss. Thus γ^2 and therefore k^2 will be real. Now we have already stated that k_2 must be complex to give correct behaviour of the Hankel function, so k_2 must, therefore, be imaginary and k_2^2 negative real.

Now $k_1^2 = \omega \epsilon_1 \mu_1 - \beta^2 = \left(\frac{\omega}{v_o}\right)^2 - \left(\frac{\omega}{v}\right)^2$

where β is the imaginary part of γ and where v_o is the velocity of plane waves in medium (1) and v is the velocity of guided waves in medium (1). As we know v must be greater than v_o, k_1^2 is thus positive and k_1 is real.

Given k_1 is real and k_2 imaginary equations (2.10) and (2.11) may be solved graphically. In Fig. 2.2 the function $x_1 \frac{J_o(x_1)}{J_o'(x_1)}$ and $x_2 \frac{H_o(x_2)}{H_o'(x_2)}$ are plotted against x_1 and x_2 on the same scales. Values of x_1 and x_2 satisfying equations (2.10) may thus be obtained from these curves. In Fig. 2.3 they are plotted in the form $x_2/i = f(x_1)$ and on the same scale is plotted the circle with centre the origin and whose equation is

$$x_1^2 + \left(\frac{x_2}{i}\right)^2 = R^2$$

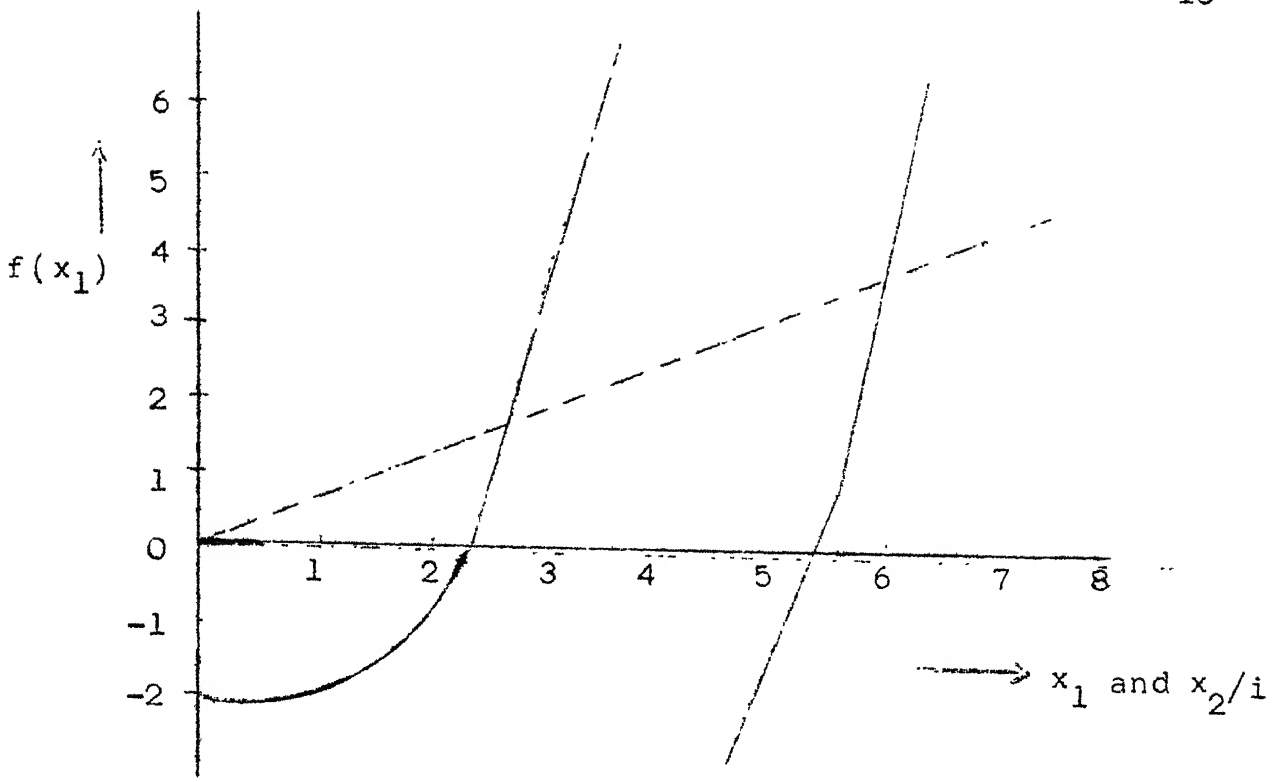

Fig. 2.2: The functions $\frac{J_o(x_1)}{J'_o(x_1)}$ and $x_2 \frac{H_o(x_2)}{H'_o(x_2)}$ (dashed)

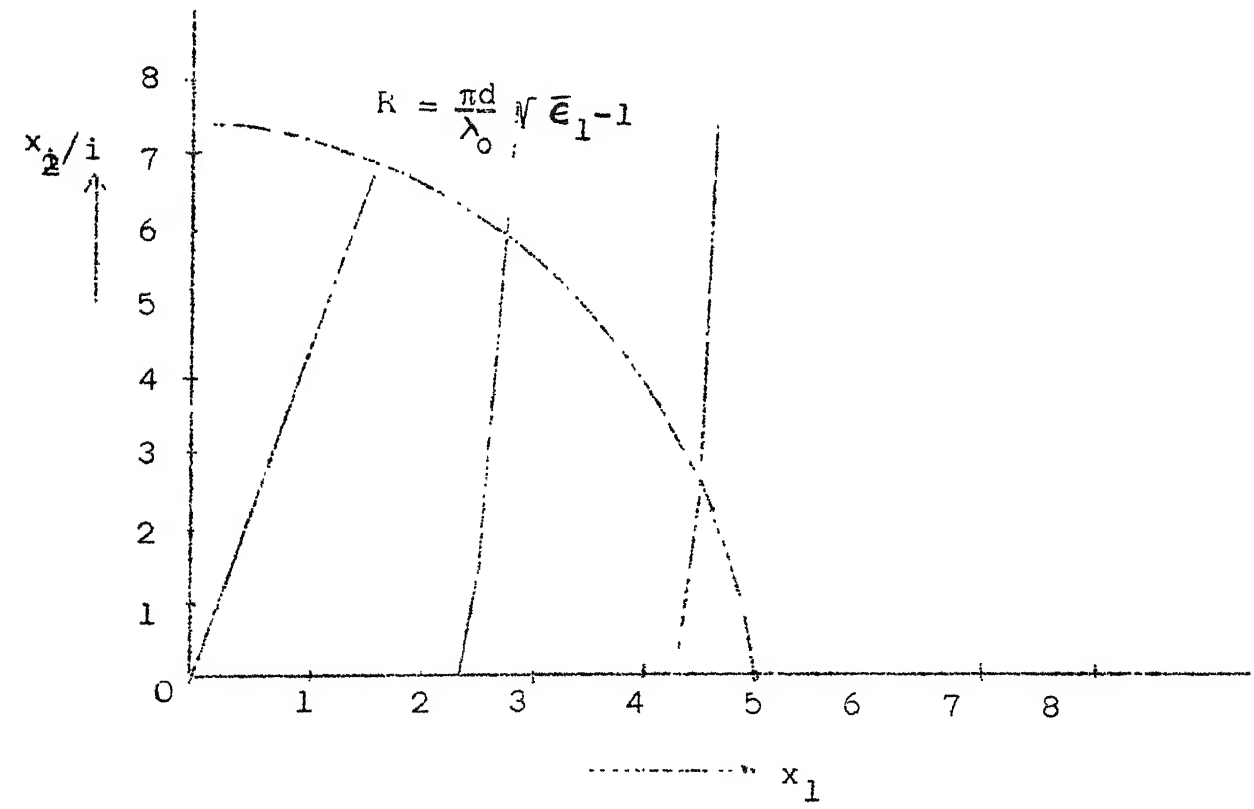

Fig. 2.3: Graphical Solution for H_{01} Waves.

The co-ordinates of the points of intersection give the values of x_1 and x_2 which fulfil both the equation depending upon the ratio $\frac{d}{\lambda_o}$ with these values the wavelength of guided wave may be obtained in the following forms

$$\left(\frac{\lambda}{\lambda_o}\right)^2 = \frac{1}{1 - \frac{x_2^2}{x_1^2 - x_2^2}(\bar{\epsilon} - 1)} = \frac{1}{1 - x_2^2\left(\frac{\lambda_o}{\pi d}\right)^2}$$

$$= \frac{1}{1 - x_1^2\left(\frac{\lambda_o}{\pi d}\right)^2}$$

This equation is shown graphically in Fig. 2.4.

It will be noted that for this axially symmetric mode propagation along the rod is impossible without radial dissipation of energy (radiation) for cylinder diameters less than a limiting diameter and for wavelengths greater that a corresponding limiting wavelengths dependent on dielectric constant and magnetic permeability. This cut off behaviour is present in the case of axially symmetric modes - there is no cut off with asymmetric hybrid HE_{11} mode which will be treated in the following section.

Immediately above this limiting value of d/λ_o the wavelength of the guided wave is almost equal to the wavelengt in the vaccum of the exciting oscillation. In consequence of the behaviour of the Hankel function, the field in the outer space dies away very slowly and only a small part of the energy flow takes place within the cylinder.

With greater value of d/λ_o, the wavelength of the guidec wave becomes smaller and approaches the value $\lambda_o/\sqrt{\epsilon_1}$. As the argument increases, the Hankel function decreases rapidly and the energy transfer tends rapidly to become totally within the cylinder.

As there is only one component of electric field (E_ϕ) the electric lines are concentric circles centred on the axis. The magnetic lines are determined by the components H_ρ and H_z; they link the electric lines chain-wise and lie fundamentally in longitudinal planes.

2.2.2 Case 2: E_{01} Waves:

By similar process as outlined above the E_{01} mode may be analysed and principal results only will be given here.

The two determining equations for the propagation constant when

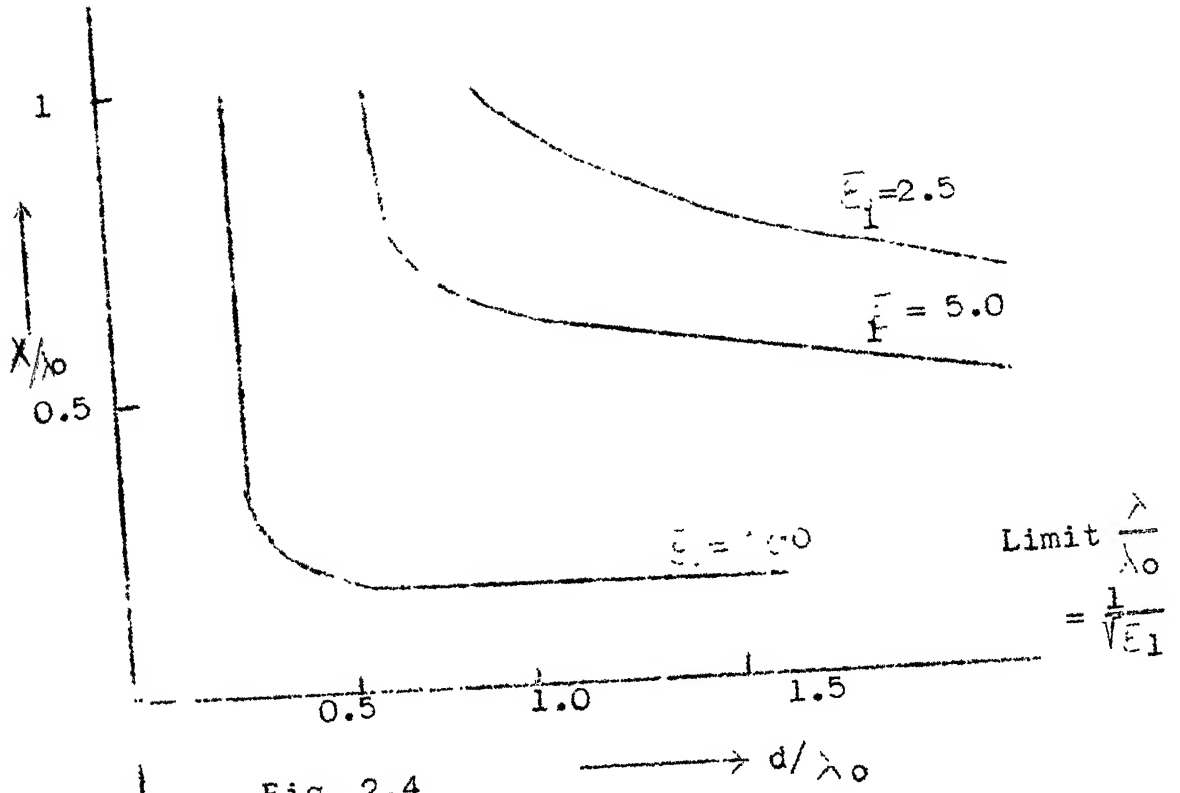

Fig. 2.4

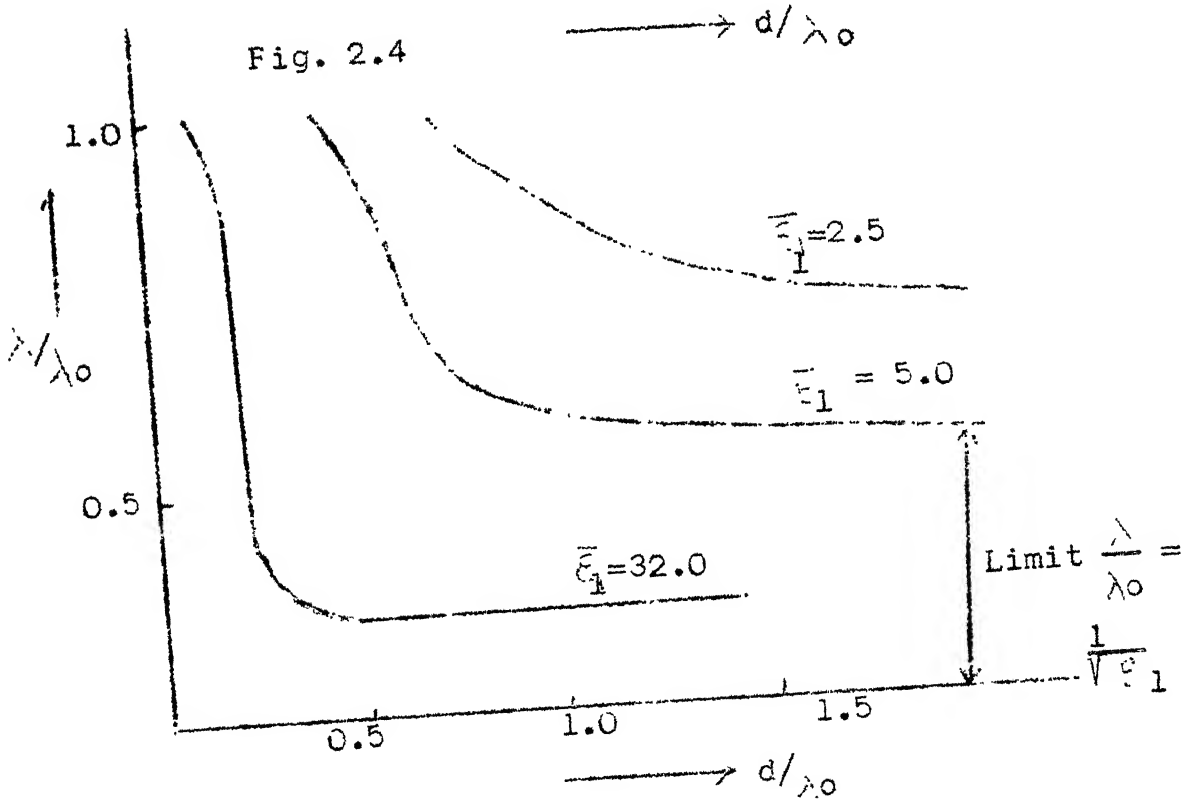

Fig. 2.5: Wavelength of E_{01} wave in relation to d/λ_o

$$\epsilon_2 = \bar{\mu}_1 = \bar{\mu}_2 = 1$$

are $$x_1 \frac{J_o(x_1)}{J_o'(x_1)} = \epsilon_1 x_2 \frac{H_o(x_2)}{H_o'(x_2)}$$

and $$x_1^2 + \left(\frac{x_2}{i}\right)^2 = \left(\frac{\pi d}{\lambda_o}\right)^2 (\bar{\epsilon}-1)$$

These are solved in the same manner as for case 1 and shape of the curves of λ/λ_o plotted against d/λ_o are very similar to those in the case of H_{01} wave. They are shown in Fig. 2.5.

It can be seen here also that there is a cut off phenomenon as before and the division of the wave energy between the cylinder and the outer space follows the same general behaviour; with large values of d/λ_o the energy is mainly confined within the rod and as d/λ_o decreases more energy is propagated in the outer space.

The magnetic field lines are concentric circles centred on the axis and the electric field lines link them in chain like manner and lie mainly in longitudinal planes.

2.3 NON-CIRCULARLY SYMMETRIC WAVES:

If propagation arises due to excitation by an asymmetric source, such as a dipole perpendicular to the axis, the mode will not possess radial symmetry of field distribution.

Consider the general case of excitation by an asymmetrical wave for which the phase around the circumference of

the cylinder changes its sign n times, then the expression for the vector potential must exhibit a corresponding dependence on parameter ϕ. So we put for the electric vector-potential

$$A^E = A_z^E(\rho) \begin{matrix}\cos n\phi \\ \sin n\phi\end{matrix} e^{-\gamma z}$$

with the same stipulation as before that (1) the field within the rod must remain finite when $\rho = 0$ and (2) the field outside the rod tends to zero as $\rho \to \infty$, the wave equation gives the solutions

$$A_1^E = B\, J_n(k_1\rho) \begin{matrix}\cos n\phi \\ \sin n\phi\end{matrix} e^{-\gamma_1 z} \qquad \text{when } \rho < r$$

$$A_2^E = C\, H_n(k_2\rho) \begin{matrix}\cos n\phi \\ \sin n\phi\end{matrix} e^{-\gamma_1 z} \qquad \text{when } \rho > r \qquad (2.12)$$

where H_n is the Hankel function of the first kind.

For the excitation of the rod by a vertical probe ($\phi = \pi/2$) Fig. 4.1, or dipole Fig. 4.2 or by a circular metal guide Fig. 4.3 carrying the H_{11} mode with electric lines predominantly vertical the E_ϕ component of the electric field in the rod must be zero when $\phi = \pi/2$. So fixing the zero of the ϕ axis we then put

$$A^{E} = A_z^{E}(\rho) \cos n\phi \; e^{-\gamma z}$$

and

$$A^{H} = A_z^{H}(\rho) \sin n\phi \; e^{-\gamma z}$$

to satisfy this condition. The field components may be obtaine by differentiating as before and H wave may be obtained.

If we proceed as before and obtain from the boundary conditions and conditional equation to determine the unknown we find that we have more equations and we can not find the solution by assuming that an H wave can exist alone. If, however, we super impose an auxiliary E wave with H wave, the boundary conditions may then be satisfied and we have a hybrid HE mode.

Now if the H and E modes are to be combined in a simple manner to form a hybrid HE mode then the propagation constants of the two waves must be equal ($\gamma_1^{E} = \gamma_1^{H}$ and $\gamma_2^{E} = \gamma_2^{H}$) and also ($k_1^{E}=k_1^{H}$ and $k_2^{E} = k_2^{H}$). Thus the field components of our postulated hybrid HE mode are obtained by adding the corresponding field components of the two waves as under:

$$E_\rho = -B\left[\frac{n}{\rho} J_n(k_1\rho) + \frac{b}{B}\frac{\gamma_1 k_1}{j\omega\epsilon_1} J_n'(k_1\rho)\right]\sin n\phi\, e^{-\gamma_1 z}$$

$$E_\phi = -B\left[k_1 J_n'(k_1\rho) + \frac{b}{B}\frac{n\gamma_1}{\rho j\omega\epsilon_1} J_n(k_1\rho)\right]\cos n\phi\, e^{-\gamma_1 z}$$

$$E_z = B\cdot\frac{b}{B}\frac{k_1^2}{j\omega\epsilon_1} J_n(k_1\rho)\sin n\phi\, e^{-\gamma_1 z}$$

$\rho < r$

$$H_\rho = B\left[\frac{\gamma_1 k_1}{j\omega\mu_1} J_n'(k_1\rho) + \frac{b}{B}\frac{n}{\rho} J_n(k_1\rho)\right]\cos n\phi\, e^{-\gamma_1 z}$$

$$H_\phi = -B\left[\frac{n}{\rho}\frac{\gamma_1}{j\omega\mu_1} J_n(k_1\rho) + \frac{b}{B}k_1 J_n'(k_1\rho)\right]\sin n\phi e^{-\gamma_1 z}$$

$$H_z = -B\cdot\frac{k_1^2}{j\omega\mu_1} J_n(k_1\rho)\cos n\phi\, e^{-\gamma_1 z}$$

and

$$E_\rho = -C\left[\frac{n}{\rho} H_n(k_2\rho) + \frac{c}{C}\frac{n}{\rho}\frac{\gamma_2}{j\omega\epsilon_2} H_n(k_2\rho)\right]\cos n\phi e^{-\gamma_2 z}$$

$$E_\phi = -C\left[k_2 H_n'(k_2\rho) + \frac{c}{C}\frac{n}{\rho}\frac{\gamma_2}{j\omega\epsilon_2} H_n(k_2\rho)\right]\cos n\phi\, e^{-\gamma_2 z}$$

$$E_z = C\,\frac{c}{C}\frac{k_2^2}{j\omega\epsilon_2} H_n(k_2\rho)\sin n\phi\, e^{-\gamma_2 z}$$

$\rho > r$

$$H_\rho = C\left[\frac{\gamma_2 k_2}{j\omega\mu_2} H_n(k_2\rho) + \frac{c}{C}\frac{n}{\rho} H_n(k_2\rho)\right]\cos n\phi\, e^{-\gamma_2 z}$$

$$H_\phi = -C\left[\frac{n}{\rho}\frac{\gamma_2}{j\omega\mu_2} H_n(k_2\rho) + \frac{c}{C} k_2 H_n'(k_2\rho)\right]\sin n\phi\, e^{-\gamma_2 z}$$

$$H_z = -C\,\frac{k_2^2}{j\omega\mu_2} H_n(k_2\rho)\cos n\phi\, e^{-\gamma_2 z}$$

Applying the boundary conditions which demand continuity of E_z, H_z, E_ϕ and H_ϕ and putting, as in the case of auxiallary symmetric modes, $\gamma_1=\gamma_2=\gamma$ because for a single hybrid wave mode to exist its propagation constant must be the same on each side of the boundary, four determining equations follow

$$b \frac{k_1^2}{j\omega\epsilon_1} J_n(k_1 r) = c \frac{k_2^2}{j\omega\epsilon_2} H_n(k_2 r)$$

$$B \frac{k_1^2}{j\omega\mu_1} J_n(k_1 r) = C \frac{k^2}{j\omega\mu_2} H_n(k_2 r)$$

$$B\, k_1 J_n'(k_1 r) + b \frac{n}{\gamma} \frac{\gamma}{j\omega_1} J_n(k_1 r) = C\, k_2 H_n'(k_2 r) + c \frac{n}{\gamma} \frac{\gamma}{j\omega\epsilon_2} H_n(k_2 r) \quad (2.13)$$

$$B \frac{n}{r} \frac{\gamma}{j\omega\mu_1} J_n(k_1 r) + bk_1 J_n'(k_1 r) = C \frac{n}{r} \frac{\gamma}{j\omega\mu_1} H_n(k_2 r) + Ck_2 H_n'(k_2 r) \quad (2.14)$$

From above first two equations we obtain equations relating the field strengths of same mode (E and H) inside and outside the cylinder.

Putting $x_1 = k_1 r$ and $x_2 = k_2 r$

we have

$$\frac{C}{B} = \frac{x_1^2}{x_2^2} \frac{\mu_2}{\mu_1} \frac{J_n(x_1)}{H_n(x_2)}$$

$$\frac{c}{b} = \frac{x_1^2}{x_2^2} \frac{\epsilon_2}{\epsilon_1} \frac{J_n(x_1)}{H_n(x_2)}$$

From (2.13) and (2.14), the relative magnitudes of thetwo modes are obtained

$$\frac{b}{B} = \frac{j\omega}{n\gamma}\frac{\epsilon_1}{\mu_1}\frac{x_1^2x_2^2}{x_1^2-x_2^2}\left[\frac{\mu_1}{x_1}\frac{J_n'(x_1)}{J_n(x_1)} - \frac{\mu_2}{x_2}\frac{H_n'(x_2)}{H_n(x_2)}\right.$$

$$= \frac{n\gamma}{j\omega}\frac{\epsilon_1}{\mu_1}\frac{x_1^2-x_2^2}{x_1^2x_2^2}\frac{1}{\frac{\epsilon_1}{x_1}\frac{J_n'(x_1)}{J_n(x_1)} - \frac{\epsilon_2}{x_2}\frac{H_n'(x_2)}{H_n(x_2)}}$$

$$= -\frac{n^2\gamma^2}{\omega^2}\left(\frac{x_2^2-x_1^2}{x_1^2x_2^2}\right)$$

Putting $\bar{\mu} = \frac{\mu}{\mu_o}$ and $\bar{\epsilon} = \frac{\epsilon}{\epsilon_o}$ and $\epsilon_2 = \bar{\mu}_2 = \bar{\mu}_1 = 1$ and n=1 RHS of the above equations may be slightly modified to make the form more convenient. The final form of the equations is as under

$$\left[\frac{1}{x_1}\frac{J_n'(x_1)}{J_n(x_1)} - \frac{1}{x_2}\frac{H_n'(x_2)}{H_n(x_2)}\right]\left[\frac{\epsilon_1}{x_1}\frac{J_n'(x_1)}{J_n(x_1)} - \frac{1}{x_2}\frac{H_n'(x_2)}{H_n(x_2)}\right]$$

$$= \frac{(x_1^2-x_2^2)(x_1^2-x_2^2\epsilon_1)}{x_1^4x_2^4} \qquad (2.15)$$

and

$$x_1^2+\left(\frac{x_i}{i}\right)^2 = \left(\frac{\pi d}{\lambda_o}\right)^2(\bar{\epsilon_1} - 1) \qquad (2.16)$$

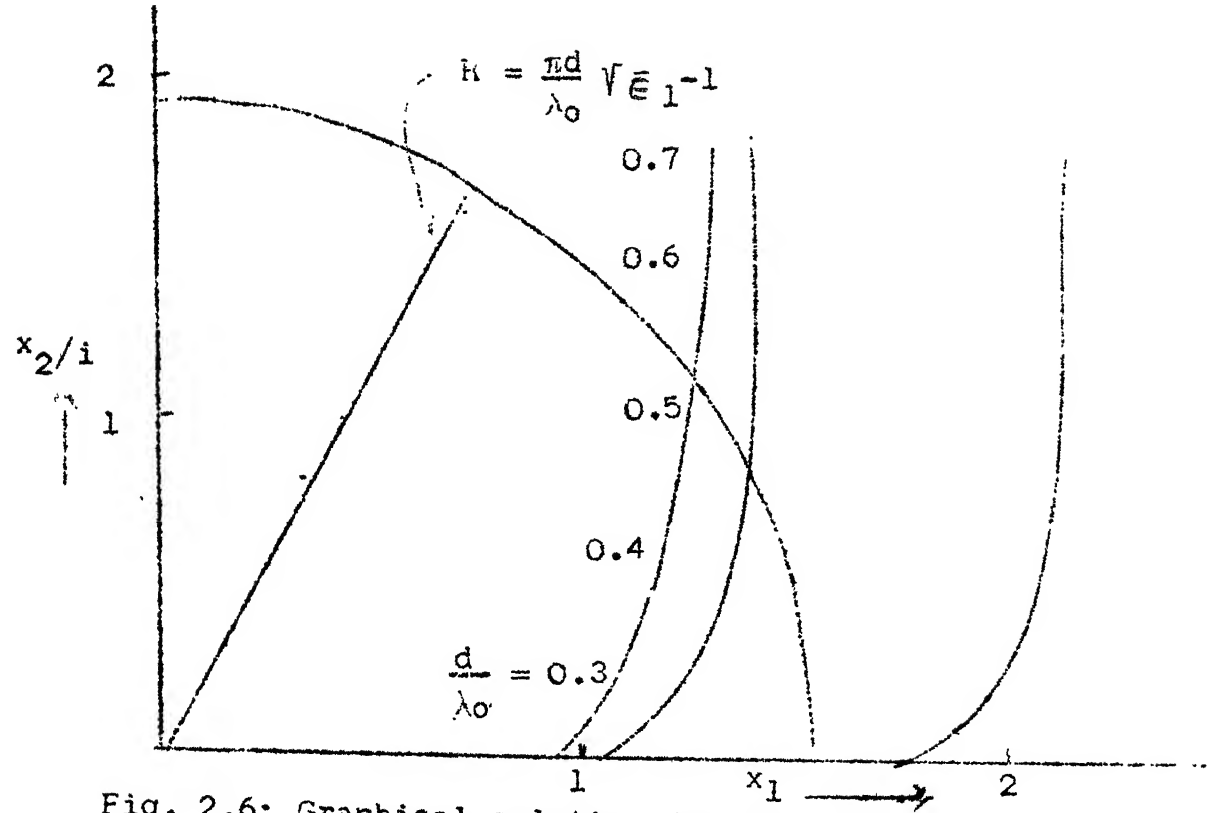

Fig. 2.6: Graphical solution for HE_{11} wave

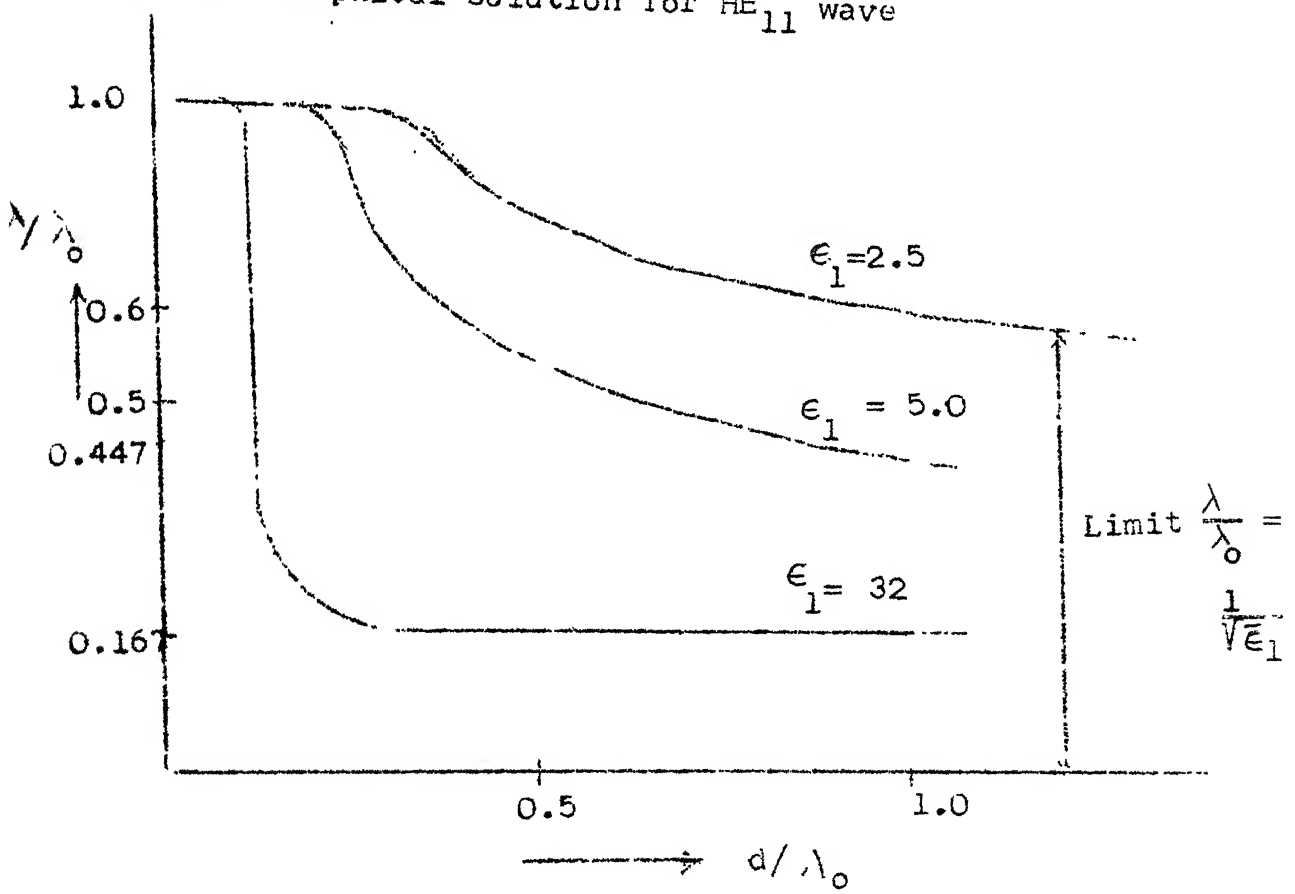

Fig. 2.7: Wavelength of HE_{11} wave as function of d/λ_o

These equations are solved graphically in a similar manner to that used for H_{01} wave. Equation (2.16) must be expressed in form $\frac{x_2}{i} = f(x_1)$ and on the same scale a circle o radius $(\frac{\pi d}{\lambda})\sqrt{\epsilon_1 - 1}$ with centre as origin is also drawn. The points of intersection give the values of x_1 and x_2, which satisfy equations (2.15) and (2.16). For each value of ϵ_1 and $\frac{d}{\lambda_o}$. This is plotted in Fig. 2.6. These values of x_1 and x_2 determine the wavelength of the guided wave.

In Fig. 2.7 the final curves of λ/λ_o plotted against d/λ_o for different values of ϵ_1 are shown for HE_{11} mode.

It will be noted that there is no cut off for this mode (but there is cut off with the higher order asymmetric modes). With small values of d/λ_o the value $\frac{\lambda}{\lambda_o}$ is sensibly unity and major part of the wave energy travels outside the rod. With larger values of d/λ_o, the value of λ/λ_o decreases a and finally approaches asymptotically the value $1/\sqrt{\epsilon_1}$ and power is transferred more and more within the rod.

For HE_{11} wave, the electric field in a transverse plane normal to the axis has the same phase and one preferred diirection which is parallel to the exciting dipole (A dipole or probe is normally used to excite the mode, the H_{11} mode in a metal guide may also be used). It is this phase quality and almost parallel nature of the field lines which make

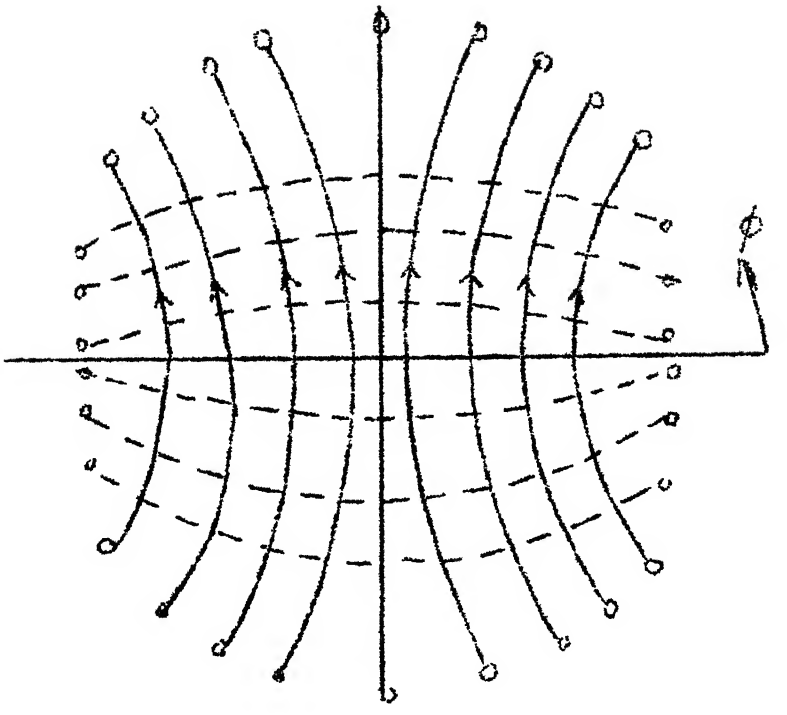

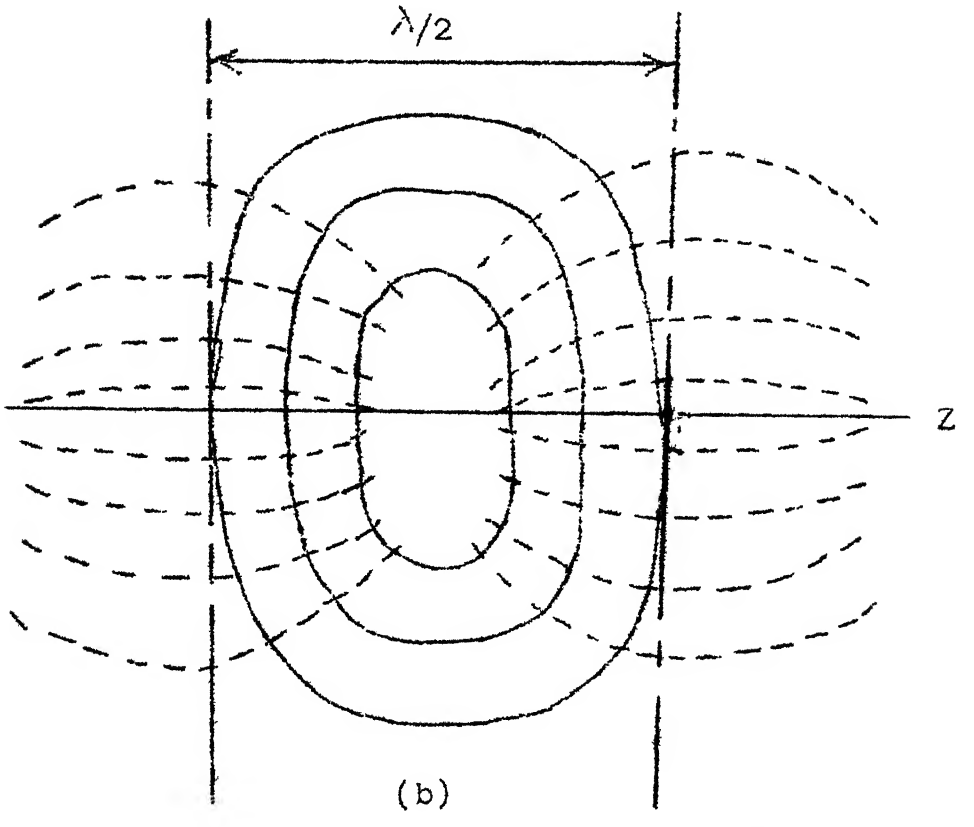

Fig. 2.8: Field distribution of HE_{11} mode

a) Transverse Section
b) Longitudnal Section

this mode in a dielectric rod, suitable for use as a directional radiator. With other types of wave modes the phase and direction of the field strength in a transverse plane change, which results in multilobed patterns, majority of which possess a null in forward (axial) direction. These modes are, therefore, unsuitable for single lobed directional radiators. The field lines of the HE_{11} mode are shown in Fig. 2.8 for both transverse and longitudinal planes.

2.3 SALIENT FEATURES OF THE PROPAGATION ALONG DIELECTRIC ROD:

Some of the principal characteristics of wave propagation along a dielectric rod have been described in the foregoing paragraphs and essential differences between the H_{om} and E_{om} modes which can exist separately and the hybrid asymmetric HE mode of which HE_{11} mode is most suitable for the directional radiator, have been brought out. This will enable the general properties of the wave modes in dielectric rods to be appreciated before proceeding to the radiation characteristics of dielectric rod aerials.

From the analysis of the propagation properties of dielectric rods while excited in various modes, one most important fact which clearly stands out is that if the

dielectric rod $\angle^{\text{antenna}}$ is properly dimensioned, it starts radiating rather than purely propagating. While designing the dielectric rod $\angle^{\text{antenna}}$ this single factor of precise dimensions (more particularly the rod diameter) are most essential.

CHAPTER 3

RADIATION OF DIELECTRIC ROD ANTENNAS

3.1 GENERAL:

It has been amply clear, from the analysis presented in Chapter 2, that if the dielectric rod is properly dimensioned it starts behaving as a radiator of electromagnetic energy. Practically all the experimental and theoretical work on dielectric rod antennas carried out till date, has been devoted to the study of the radiation pattern characteristics and derivation of mathematical expressions to describe them. The problem of radiation characteristics of dielectric rod antennas is much less amenable to precise mathematical treatment than the propagation of a wave along a rod as will be seen in the following study.

The main bulk of theoretical work devoted to the radiation pattern characteristics has produced three different methods of approach.

3.2 THREE DIFFERENT HYPOTHESIS OF RADIATION:

3.2.1 Huyghens Principle Method:

It is relatively simple and straightforward. It is based on elementary ray theory and provides an expression which contains the parameters; rod diameter, rod length,

dielectric constant and wavelength and is applicable to rod excited in HE_{11} mode. This expression describes the variations in the main lobe of the pattern with a fair degree of success but it is quite inadequate in describing the side lobes structure which is most important test of adequacy of radiation pattern expression. Although it is an over simplification of the problem and of only limited application to the main lobe of pattern, the Huyghens principle approach provides a simple expression which is nevertheless of value in some practical applications.

3.2.2 'Wavelength Lens' Approach:

The second method interprets the dielectric rod antennas as a type of lens; the term 'wavelength-lens' is used, and some interesting conclusions regarding the mode of operation of the antenna are arrived at. From an antenna design point of view, this theory does not add much, but it is of academic interest.

3.2.3 Schelkunoff Equivalence Principle Approach:

This method is most advanced and complete interpretation of the dielectric rod antenna that has yet appeared. It postulates a set of quite fictitious electric and magnetic surface currents in the rod from which the radiation pattern expression is derived. This expression can give main beam

and side lobe characteristics of the radiation pattern of a circular section rod excited in H_{01} mode to high degree of accuracy when an 'effective diameter' of the rod is chosen by trial to replace the actual rod diameter. The effective diameter is less than the actual diameter. The application of this theory to the radiation patterns of rods excited in HE_{11} mode is not quite so successful but, in general, the analysis is the most satisfactory yet developed.

3.3 DERIVATION OF RADIATION PATTERN EXPRESSION (BY SCHELKUNOFF EQUIVALENCE PRINCIPLE APPROACH)

This approach by WATSON and HORTON, postulates a set of electric and magnetic currents on the surface of the rod and from the distributions of these currents to derive expressions for the electro-magnetic field at large distances from the rod. Although physically quite fictitious, these surface currents provide a useful tool with which to derive expressions for the radiation patterns of circular section dielectric rods.

When this theory is applied to circular section rods excited in H_{01} mode (a pure H mode with circular symmetry giving null in the radiation pattern in the axial direction), agreement between theory and experiment is excellent and indeed most striking when an effective rod diameter which is less than the true rod diameter is chosen arbitrarily

for the evaluation of the derived radiation pattern expression. The field distributions of H_{01} mode are simpler and amenable to calculation.

The general procedure of this analysis is to calculate from the tangential components of the electric and magnetic fields at the surface of dielectric rod equivalent magnetic and electric surface currents from which the radiation pattern is computed.

When this theoretical treatment is applied to circular section rods excited in pure H_{01} mode, which gives a null in the axial direction instead of a maximum in the radiation pattern, much greater success is obtained in agreement with experimental results when the diameter of the cylindrical surface on which the magnetic currents lie, is taken to be 0.65 of the rod diameter. Agreement between theoretical and experimental results under these conditions is excellent as can be seen from Fig. 3.1 where radiation patterns are plotted for the full 360° for an untapered rod six wavelength long and 0.87 wavelengths diameter. This is due to . more accurate knowledge available for the field distribution of the symmetric, pure H_{01} mode and the agreement is true for all rod lengths except very short rods(less than two wavelengths long)where the

Theoretical Experimental

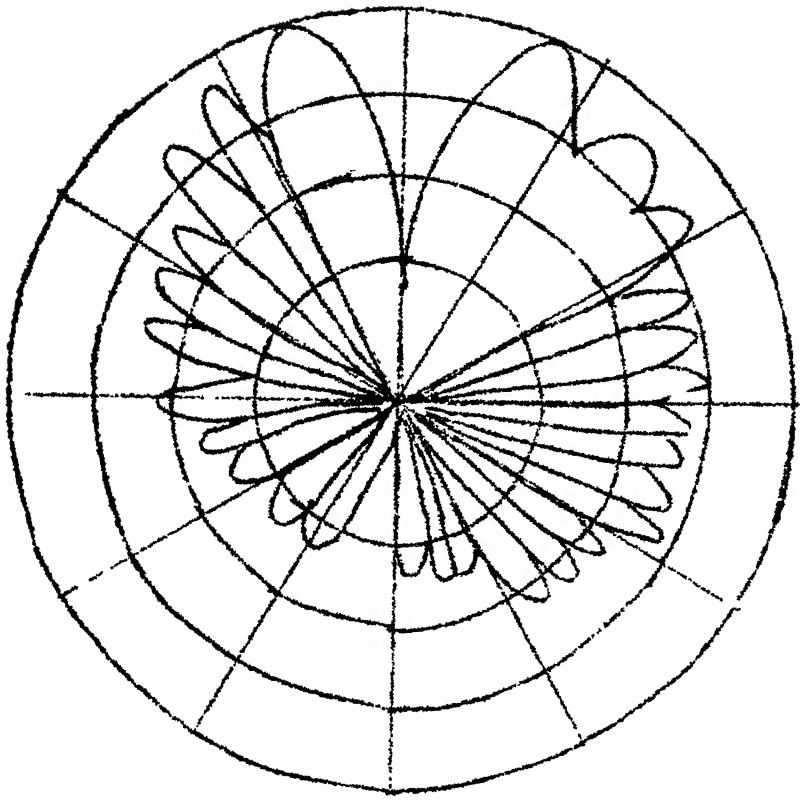

Fig. 3.1: The experimental and theoretical patterns of a lucite rod 6 λ_o log and 0.87 λ_o in diameter.

field radiated by the end of the rod is not negligible compared to field radiated by the cylindrical surface. The choice of the effective rod diameter is, however, arbitrary, in that it is chosen to give best agreement between theory and experiment. The electromagnetic field in a circular section rod excited in the H_{01} mode is known precisely and the Equivalence Principle may be directly applied.

The Equivalence Principle states that 'The electromagnetic field, inside a surface Σ due to sources outside the surface, can be produced by sheet electric current J and sheet magnetic current M over Σ given by

$$J = -n \times H^{o}$$

$$M = n \times E^{o}$$

where n is a unit normal vector directed outwards from Σ and E and H are values of E and H on the surface Σ'.

In terms of these equivalent currents, the magnetic and electric vector potentials at a point P within Σ are given by

$$A^H = \frac{1}{4\pi} \int_{\Sigma} J \frac{e^{ikr'}}{r'} d\Sigma$$

$$A^E = \frac{1}{4\pi} \int_{\Sigma} M \frac{e^{ikr'}}{r'} d\Sigma$$

where r' is the distance from $d\Sigma$ to P and $k = \frac{2\pi}{\lambda_o}$

The electric and magnetic fields at P under these conditions

$$E = j\omega\mu A^H - \frac{1}{j\omega\epsilon} \text{ grad div } A^H - \text{Curl } A^E$$

$$H = j\omega\epsilon A^E - \frac{1}{j\omega\mu} \text{ grad div } A^E + \text{Curl } A^H$$

If E^o and H^o are known, the above six equations enable the radiation pattern of dielectric rod to be calculated.

3.4 RECENT THEORETICAL METHODS FOR RADIATION CHARACTERISTICS:

3.4.1 Hybrid Model Approach:

In this a hybrid model solution [25] is developed for the circular semi-infinite dielectric rod antenna excited in HE_{11} hybrid mode. Numerical results for near zone and far zone fields as well as the gain, beamwidth and percentage of power radiated, are determined for rods of different diameter and dielectric constant by enclosing the rod with concentric metal pipe and allowing the radius of pipe to become large. Comparison is made between these results and previous approximate methods of solution that have been applied to dielectric antennas.

3.4.2 A Scattering Theory Approach:

A short coming of both the surface integration and the two aperture approach to the prediction of dielectric rod antenna patterns are well known. An alternative procedure based on a simplified scattering model [28] is presented in this approach which is capable of yielding satisfactory results without the necessity of making emperical corrections.

3.5 MECHANISM OF RADIATION:

When considering the dielectric rod of finite lengths as radiating systems it has been assumed that radiation takes place from the surface of dielectric while the excitation conditions were primarily those for non-radiating modes. That is, if rod was terminated by a matched transforming device similar to that at exciting end, energy would be transferred along the system with only small radiation loss, due to imperfections of the launching device. We must consider non-analytically, the mode changes which take place when the matched receiving transformer is removed and dielectric guide becomes a dielectric antenna which is still being excited in the non-radiating mode.

The requirement is to postulate a physical picture of a mechanism of radiation which will explain the following experimental observations, representing the principal radiation

characteristics of dielectric antennas:

a) The main lobe of the radiation pattern is directed along the axis of the antenna in the direction of the free end.

b) The directivity of a dielectric antenna of optimum design is proportional to the length of the rod.

c) The main lobe of the radiation pattern of a dielectric rod is more directive and side lobes are smaller (for long rods) when the rod is tapered towards the free-end.

The following mechanism of radiation is an explanation of the experimental observations. The non-radiating-mode (usually HE_{11}) is launched on the rod by the feed system and is accompanied by some slight radiation due to imperfections of the mode transformation at the feed. The waves in this mode travel to the free end of the antenna where some radiation to free space takes place and reflections occur. The radiation characteristics at this point are entirely a function of the mode and dimensions of the free end of the rod and are independent of antenna length. The reflection is of a complex nature, in that the original mode is not only reflected but a numbers of radiating modes are generated at the end discontinuity and propagated back along the antenna towards the feed. The proportion of energy reflected in the non-radiating mode is probably small as the end boundary is

unsuitable for this reflection being discontinuous only at the rod surface while the fields outside the rod meets no discontinuity at the end. A large metal plate normal to the axis at the end of the antenna would efficiently reflect the incident mode. The reflected energy in the original mode causes a small amplitude standing wave along the antenna and passes back into the feed which is assumed to be matched. It, therefore, does not contribute to the main radiated field of the antenna.

The radiating modes generated at the free end of the antenna travel back towards the feed end where they are reflected and they now set up a standing wave pattern on the antenna.

We thus have a system in which the net energy flow is in the direction of the free end of the antenna and radiating fields exist along the length of the rod, such a system is then amenable to more precise analysis by Schelkunoff Equivalence Principle. The net energy flow in the direction of the free end is compatible with a radiation pattern having main lobe along the axis directed away from feed.

Normal end-fire array theory applied to such a system predicts the variation of directivity with length. When the antenna is long (more than six wavelengths), the much smaller

increase of directivity with length is due to the radiating modes on the antenna being attenuated at the feed end and so causing the region near the antenna feed to be inefficiently excited as a radiator; as the length is further increased, the weakly, excited region extends further from feed and directivity is but little affected.

The fact that tapering the dielectric rod antenna improves its radiation pattern by causing main lobe to be more directive and the side lobes to be smaller is probably due to radiating modes being generated continuously along the tapered length, due to constantly changing diameter. This method of excitation presumably produces a distribution of radiation fields which is more suitable for the production of single lobed radiation pattern with small side lobes than does the excitation of the radiating modes by end discontinuity alone. Tapering of the dielectric rod to a point or to a small diameter also ensures that at the free end only the HE_{11} mode is present in the rod - the others being evanescent as the rod is beyond the cut off dimension. Under these conditions the radiating mode excited at the end is that one associated with HE_{11} mode. The diameter should be large at the excitation end to give a good match between the mode in the rod and mode in the metal cap as the energy

is contained more within the rod for thicker rods. Also a greater average diameter of the rod gives more directivity to the pattern than would a uniform cylindrical rod of smaller diameter.

The radiation mechanism explained above helps in derivation of the radiating fields in a more satisfactory manner in which end discontinuity plays an essential part.

3.6 VARIATION OF RADIATION PATTERN WITH FREQUENCY:

In this respect, in general, it is true that the pattern changes slowly with frequency. As the frequency is increased above the design frequency, the beam width decreases as one would expect but in general it is found that there is little change of general pattern characteristics for relatively very large frequency change. Hence one can predict that dielectric rod antennas are more or less broad band antennas.

CHAPTER 4

AUTOMATED MEASUREMENT OF DIELECTRIC ROD ANTENNA

4.1 GENERAL:

In the preceding chapters we have seen theoretical behaviour of the dielectric rod. Some of the modes of radiation have been described and methods of finding out the radiation characteristics have been discussed. In this chapter, automated measurement on the dielectric rod antenna (mainly radiation characteristics) have been carried out.

4.2 EXCITATION OF DIELECTRIC ROD ANTENNA:

Before we deal with the question of radiation characteristics, it is worthwhile to discuss various methods of excitation of dielectric rod antenna. These radiators may be excited by any of the following methods.

4.2.1 Excitation by Metal Waveguides:

To excite a dielectric rod antenna in a given mode it is, in general, necessary to create at the end of the rod a field configuration as closely similar to that of required mode as possible. As the field configurations of the modes in a dielectric rod are very similar to the corresponding modes in metal tube waveguides, a simple method of excitation is thus available. The metal tube guide is excited in the appropriate

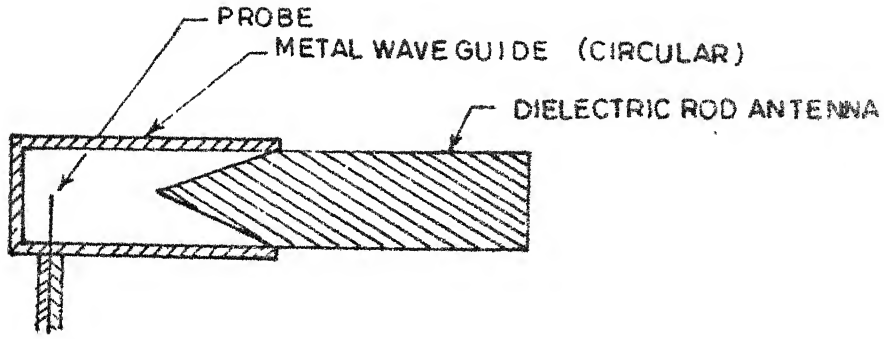

EXCITATION BY METAL WAVE GUIDE
FIG. 4·1

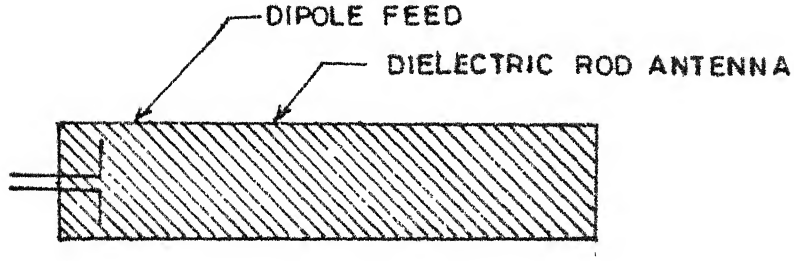

EXCITATION BY DIPOLE
FIG. 4·2

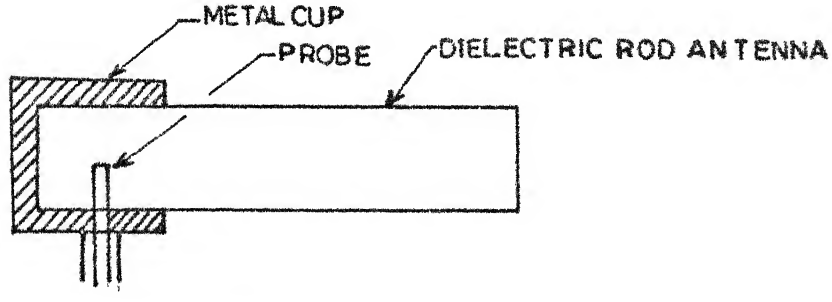

EXCITATION BY METAL CUP AND PROBE
FIG. 4·3

mode and the dielectric rod is inserted in the end of metal guide- as shown in Fig. 4.1. The position of the dielectric rod within the metal guide is tapered to a point to provide smooth transition and a degree of matching.

4.2.2 Excitation by Dipoles:

In another method of excitation which is mainly useful for thicker diameter dielectric rod antennas, a dipole is embedded inside the dielectric as shown in Fig. 4.2.

4.2.3 Excitation by Cup and Probe:

The dominant HE_{11} mode can also be excited by the metal cup and probe arrangement as shown in Fig. 4.3, as the field configuration of this arrangement is similar to that of HE_{11} mode. This method of excitation is more widely used at larger centimetric wavelengths where dielectric rod dimensions are large and concentric lines (coaxial cable) may be used for transmission over short distances. The HE_{11} mode is most often used for dielectric rod antennas and specially for experimental purposes. Therefore in our experimental set up, this method of excitation has been employed.

4.3 AUTOMATIC RADIATION PLOTTER:

As mentioned earlier that during experimental investigations of dielectric rod antenna, a great deal of difficulty

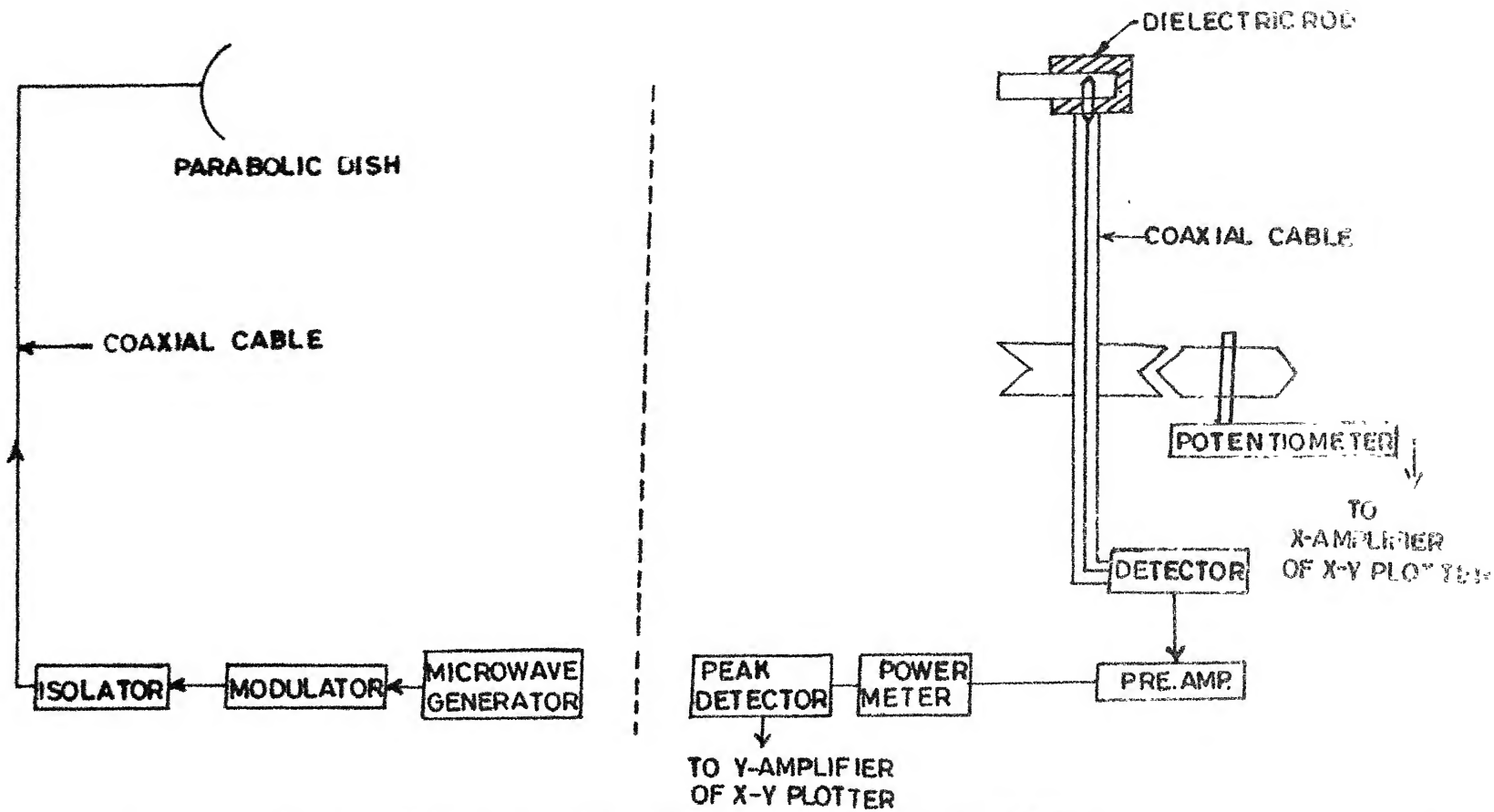

SCHEMATIC DIAGRAM OF AUTOMATIC RADIATION PLOTTER

FIG. 4.4

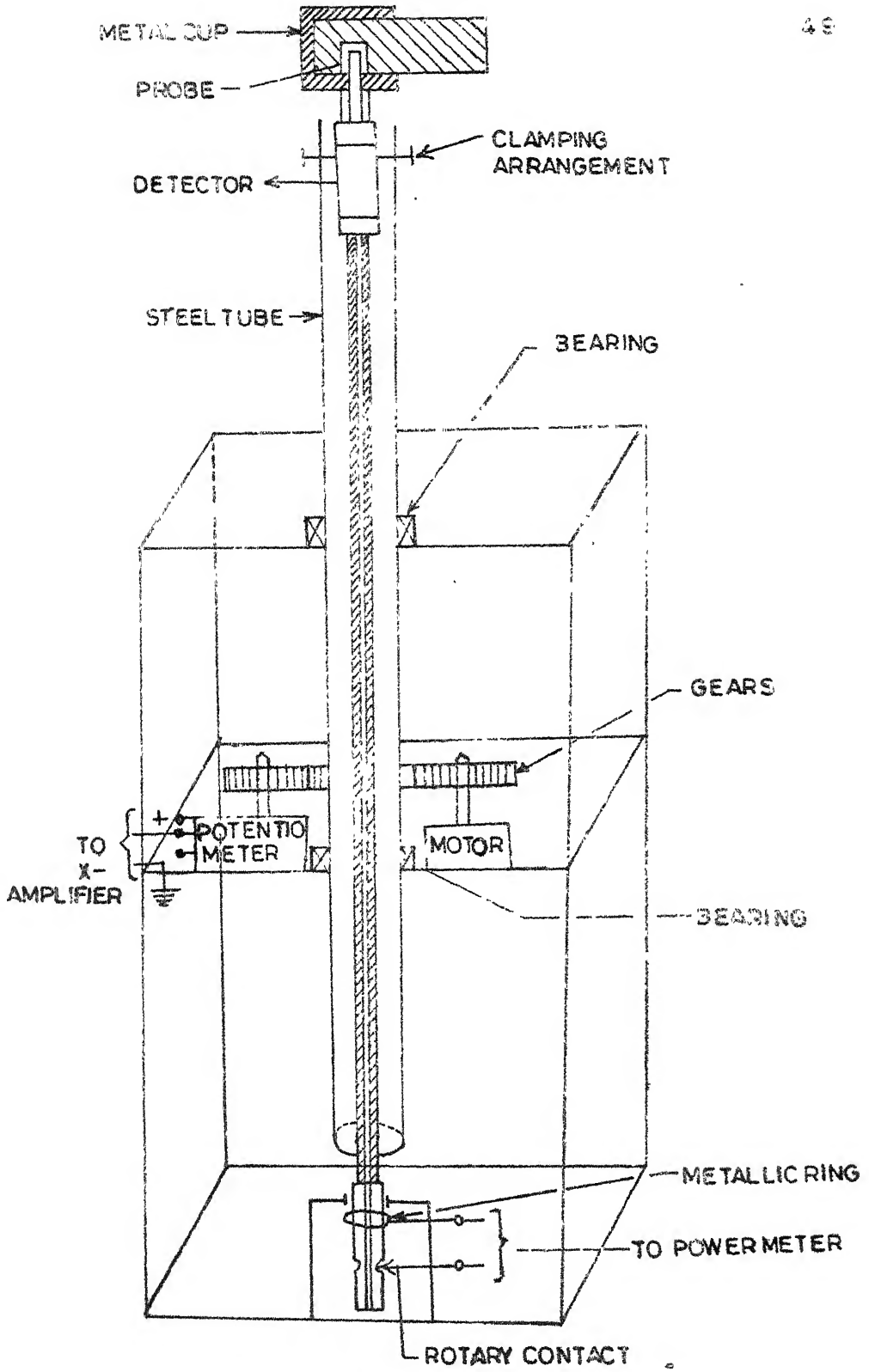

AUTOMATIC RADITION PLOTTER

FIG.4·5

was experienced due to the instability of the generator output and irregular behaviour of other testing equipments/instruments when handled manually to plot the radiation characteristics. To get reliable results a necessity was felt to use an automatic radiation plotter. In view of the foregoing, an 'Automatic Radiation Plotter' was designed and constructed. The technical details of the same are furnished in the following paragraphs.

4.3.1 Construction of Automatic Radiation Plotter:

The schematic diagram is shown in Fig. 4.4. It consists of three shelved table (4'x4'x4' size) on which a steel tube has been mounted and secured by two bearing to keep it vertical and allow it to revolve for 360° around its axis. On the top of this steel tube, antenna under test is mounted as shown in Fig. 4.5. On second shelf a two phase AC motor is mounted with gear arrangement to provide revolution to the steel tube. On the same shelf, a potentiometer arrangement with gear arrangement is mounted so that motor, steel tube and the potentiometer revolve at the same speed (gear ratio for motor, steel tube, and potentiometer axle is 1:1:1). The potentiometer linearly variable output is used to feed the X-amplifier of the X-Y plotter. Hence on X-axis we have 0° to 360° varying as per the position of the antenna.

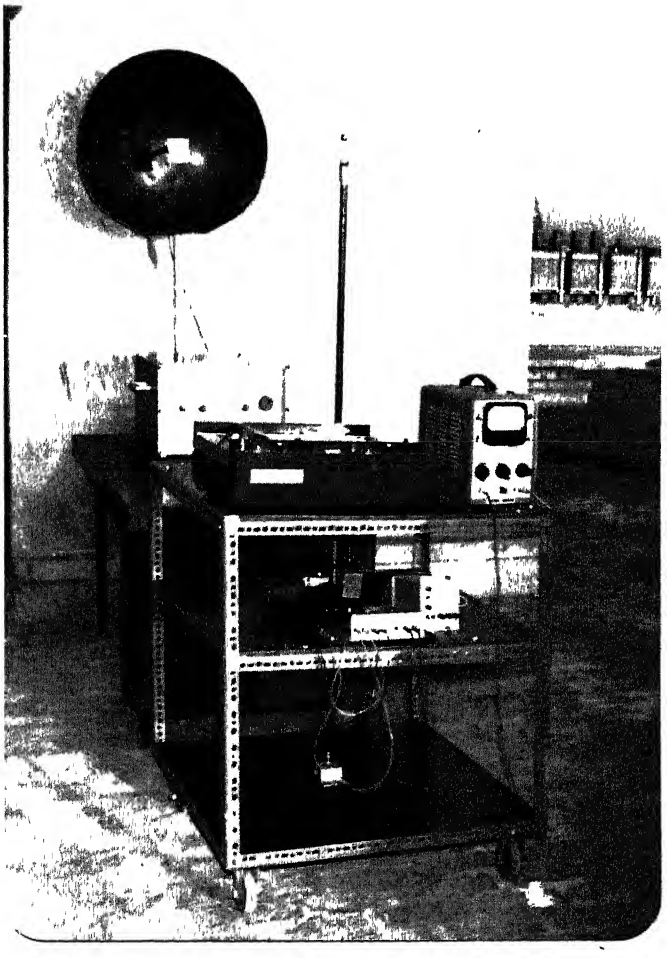

Experimental set-up

The antenna under test is excited by metal cup and probe arrangement which is most widely used for experimental purposes. The output from the antenna is fed to square law detector and 1 KHz output of detector is taken to a rotary joint arrangement from where this output is fed to a power meter for visual indication. From the recorder terminal of the power meter, this output is fed to peak detector (essentially a rectifier) which gives DC output that varies according to the field strength picked up by the antenna under test. This output is fed to Y-amplifier of the X-Y plotter. The complete system is shown in Fig. 4.5.

When the antenna revolves around its axis for 360^{o}, X-amplifier receives a linearly varying DC from the potentiometer and plotter needle moves on the X-axis where as Y-amplifier receives a DC which varies depending upon the field strength of the antenna at that position.

The automatic radiation plots (5) for different frequencies and for different diameters and lengths of the dielectric rod antenna are shown in Figs. 4.6(a) to Fig. 4.6(e).

4.4 ANALYSIS OF THE AUTOMATIC RADIATION PLOTS:

For the purpose of the analysis, the antenna material under test was Teflon ($\epsilon' = 2.1$). Twelve samples of dielectric

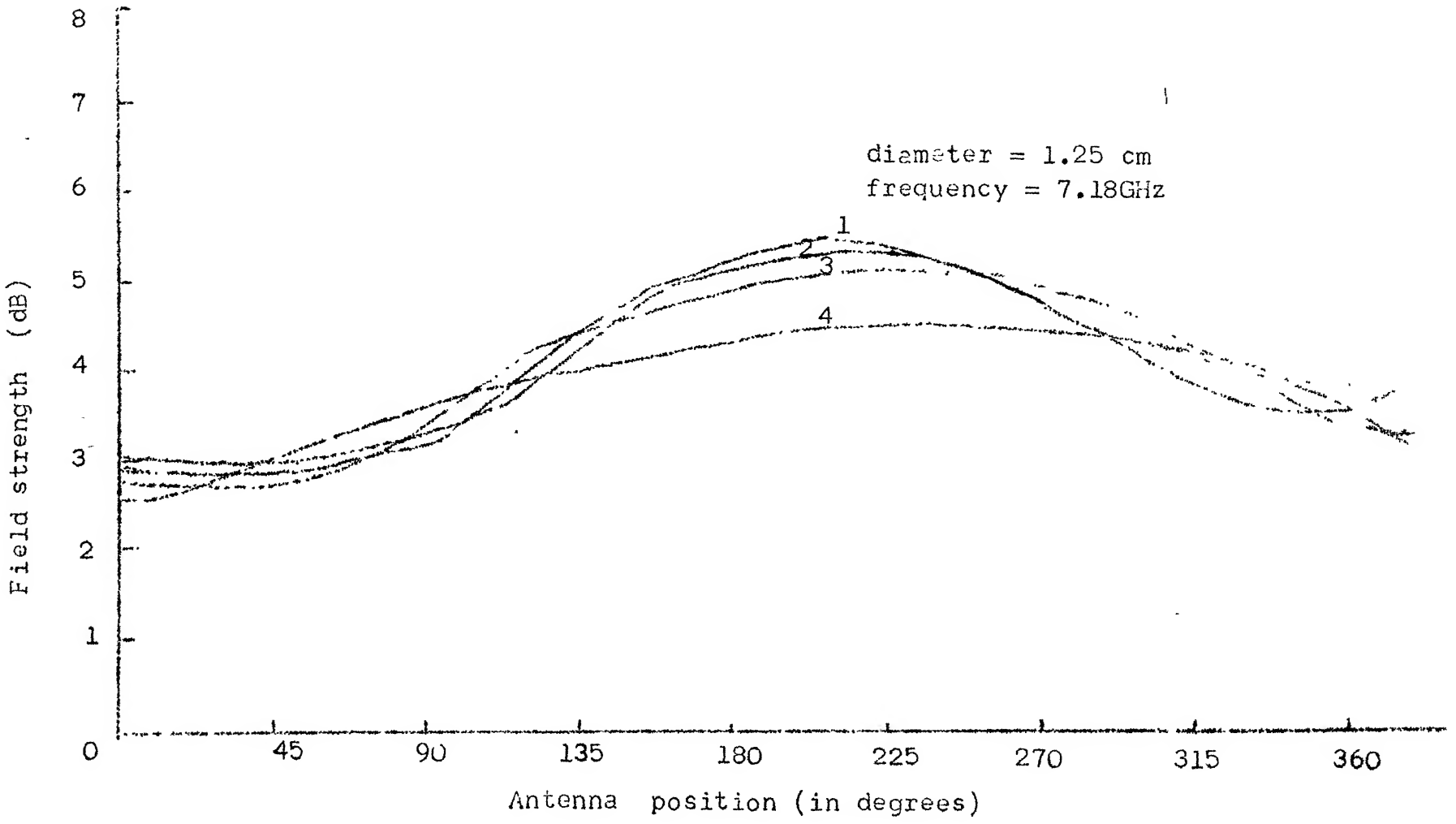

Fig. 4.6(a): Radiation Plot

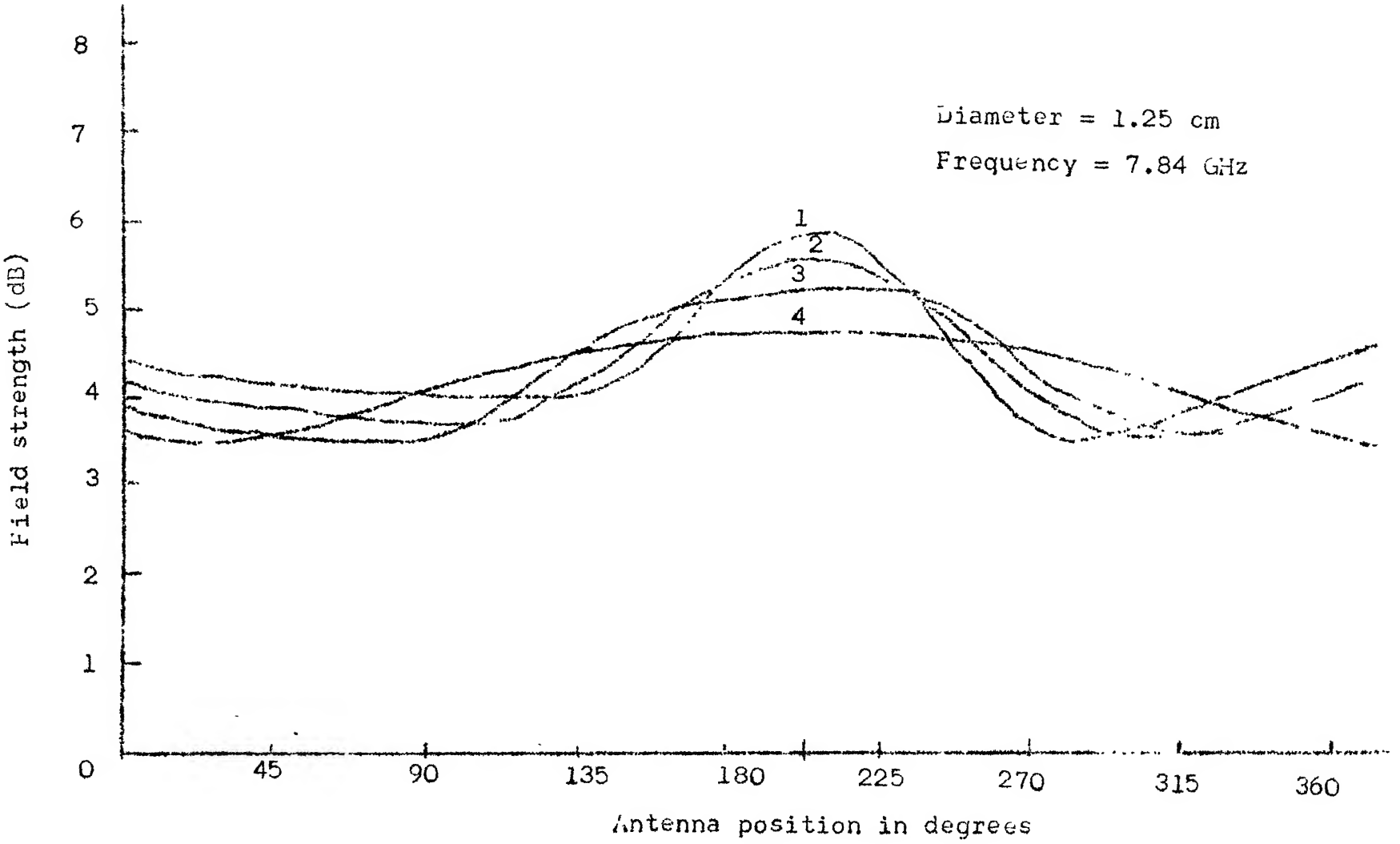

Fig. 4.6(b): Radiation Plot

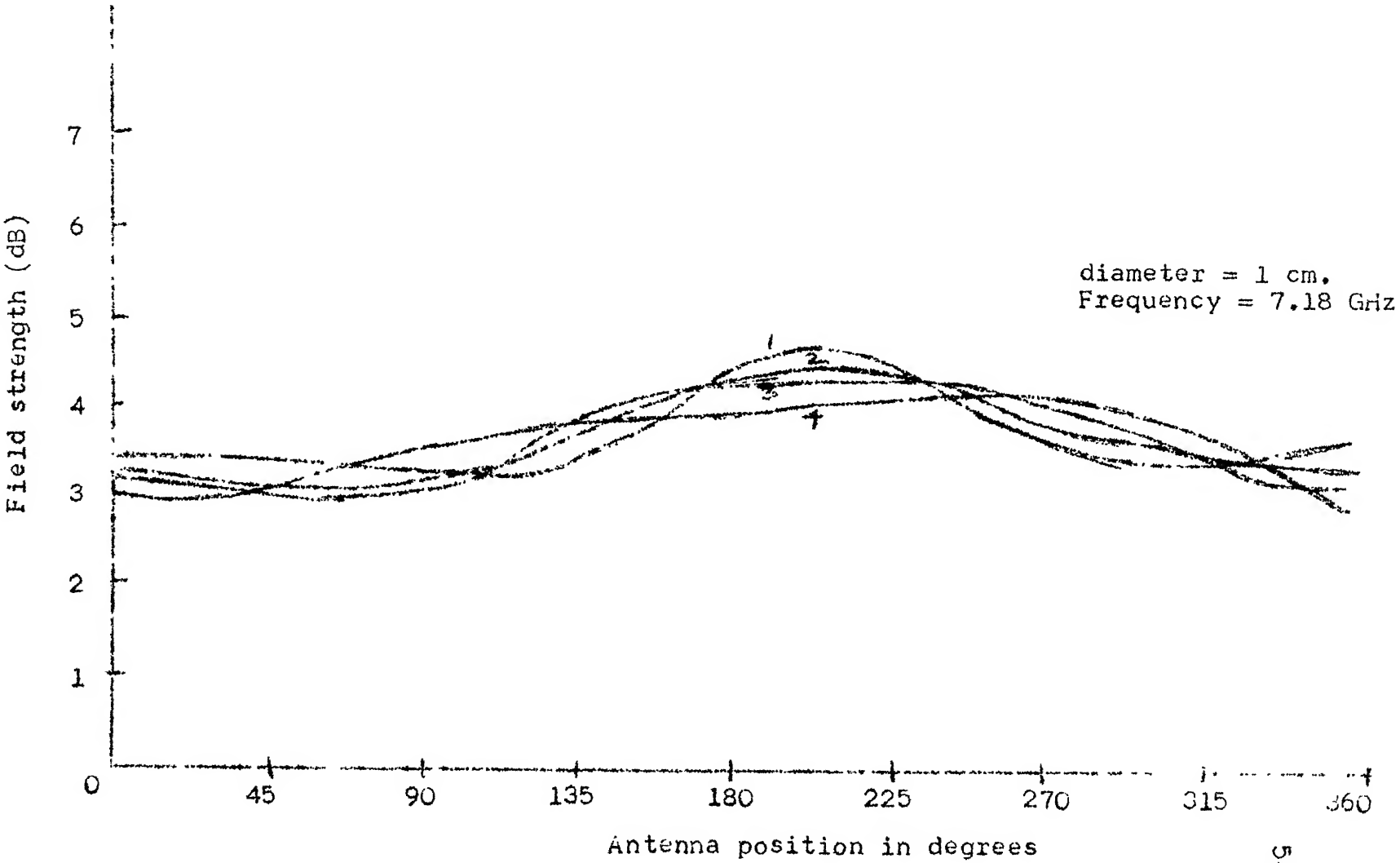

Fig. 4.6(c): Radiation Plot

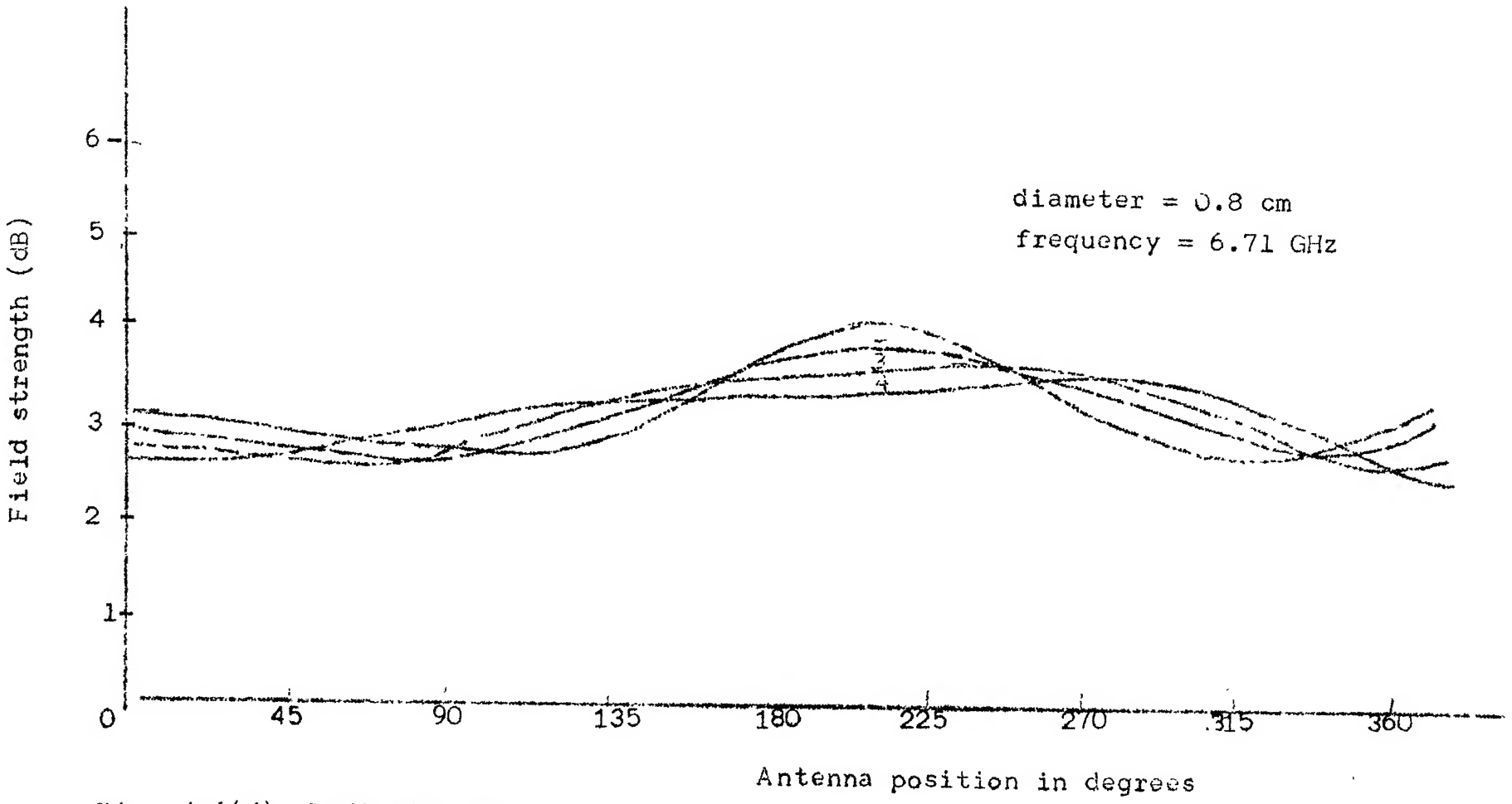

Fig. 4.6(d): Radiation Plot

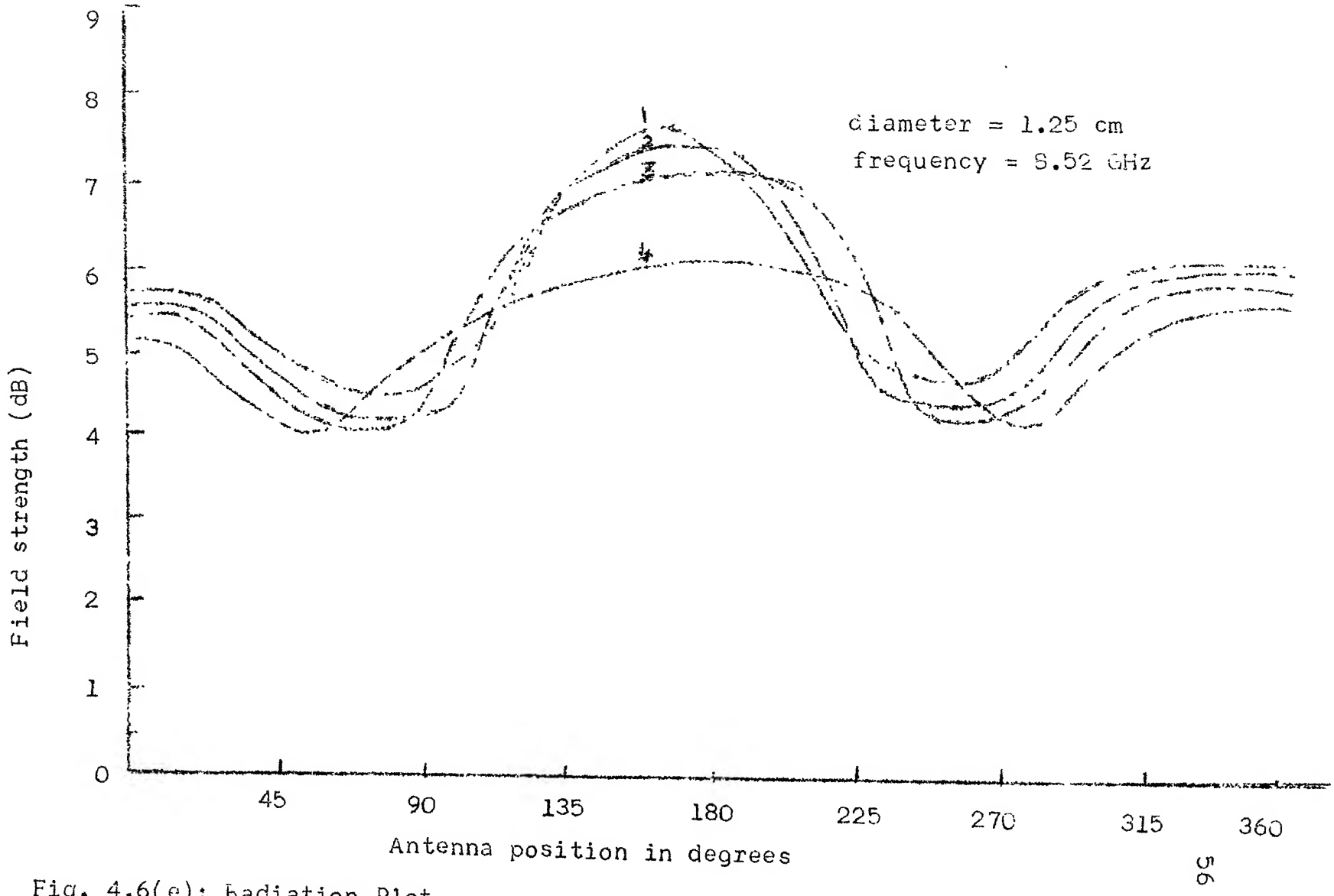

Fig. 4.6(e): Radiation Plot

rod antenna made out of Teflon were used whose diameters and lengths are as under

Diameter	Length 1	Length 2	Length 3	Length 4
12.5 mm	10.2 cm	8.3 cm	5.3 cm	2.3 cm
10 mm	10.2 cm	8.3 cm	5.3 cm	2.3 cm
8 mm	10.2 cm	8.3 cm	5.3 cm	2.3 cm

The above samples were excited at the following frequencies

i) 6.71 GHz, ii) 7.10 GHz , iii) 7.18 GHz
iv) 7.42 GHz, v) 7.70 GHz, vi) 7.84 GHz
vii) 7.94 GHz, viii) 8.10 GHz, ix) 8.14 GHz
x) 8.27 GHz, xi) 8.52 GHz

The ratio d/λ_o and L/λ_o is given in Table 1.

4.4.1 Dependence of Field Strength (main lobe) on L/λ_o and d/λ_o:

From the various radiation plots, it is seen that there is definite dependence of the ratios d/λ_o and L/λ_o on the radiation characteristics and field strength picked up (only main lobe is considered here). Generally we can conclude that main lobe amplitude increases with increase in the diameter of the rod and also the length of the rod but this relationship is not quite linear. The dependence is more prominent for the rod lengths more than $2\lambda_o$. The dependence of field strength amplitude on L/λ_o is plotted in Fig. 4.7.

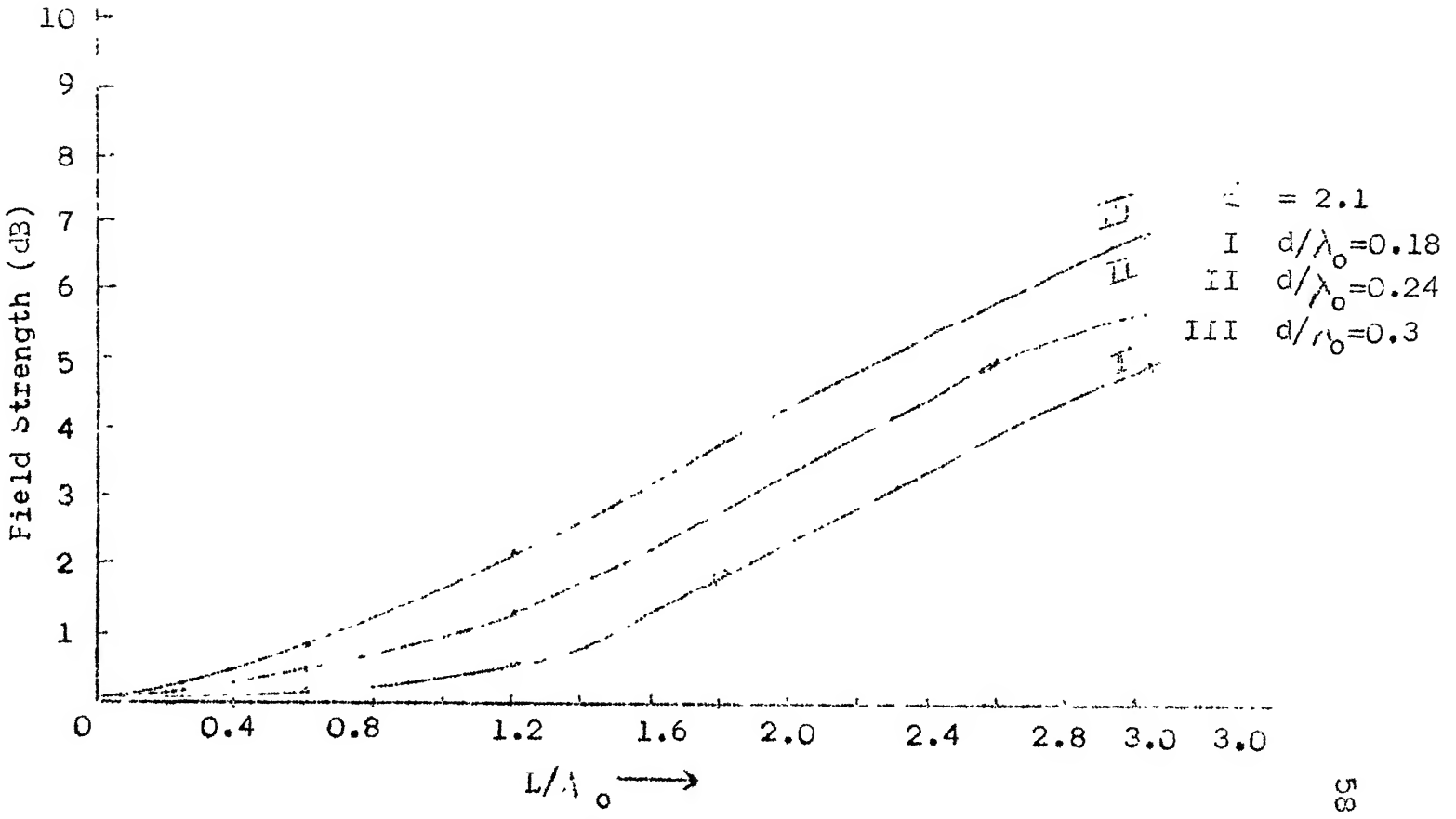

Fig. 4.7: Measured dependence of field strength (main lobe) on L/λ_o

4.2.2 Dependence of Beamwidth on L/λ_o:

As we know that dielectric rod antenna is basically a directional antenna and for design purposes it is very necessary to know the parameters that will increase its directivity. From the radiation plots it stands out quite clearly that the beamwidth between first nulls (BWFN) of this antenna is largely dependent upon the length of dielectric rod though this dependence is not linear and directivity does not increase indefinitely with increase in the length of the rod. Also, the increase in diameter of the rod too affects the directivity. Increase in the directivity with increase in rod diameter is marginal. The dependence on L/λ_o and d/λ_o is plotted in Fig. 4.8.

4.4.3 Side-lobe Dependence on L/λ_o:

The side lobe level increases as the length of the dielectric rod antenna is increased. In fact this increase is almost linear for higher d/λ_o ratio. Theoretically, it is also clear that the greater L/λ_o, the more numerous are side lobes and larger they are relative to main lobe. From the radiation characteristics plotted, it has been analysed that for different diameters of the rod, side lobe level is different for different length. This has been plotted on Fig. 4.9.

Table 1

Freq. (in GHz)	λ_o	L_1/λ_o	L_2/λ_o	L_3/λ_o	L_4/λ_o	d_1/λ_o	d_2/λ_o	d_3/λ_o
6.71	4.47	2.304	1.856	1.185	0.514	0.28	0.22	0.179
7.10	4.23	2.434	1.962	1.252	0.543	0.29	0.23	0.189
7.18	4.18	2.464	1.985	1.267	0.55	0.3	0.24	0.191
7.42	4.04	2.549	2.054	1.311	0.569	0.31	0.25	0.198
7.70	3.9	2.641	2.128	1.358	0.589	0.32	0.26	0.205
7.84	3.83	2.689	2.167	1.383	0.6	0.33	0.26	0.208
7.94	3.78	2.724	2.195	1.402	0.608	0.33	0.265	0.212
8.10	3.7	2.783	2.243	1.432	0.621	0.34	0.27	0.216
8.14	3.68	2.799	2.255	1.440	0.625	0.35	0.272	0.217
8.27	3.62	2.845	2.292	1.464	0.635	0.355	0.28	0.22
8.52	3.52	2.926	2.357	1.505	0.653	0.36	0.29	0.227

L_1 = 10.2 cm
L_2 = 8.3 cm
L_3 = 5.3 cm
L_4 = 2.3 cm

d_1 = 1.25cm
d_2 = 1 cm
d_3 = .8 cm

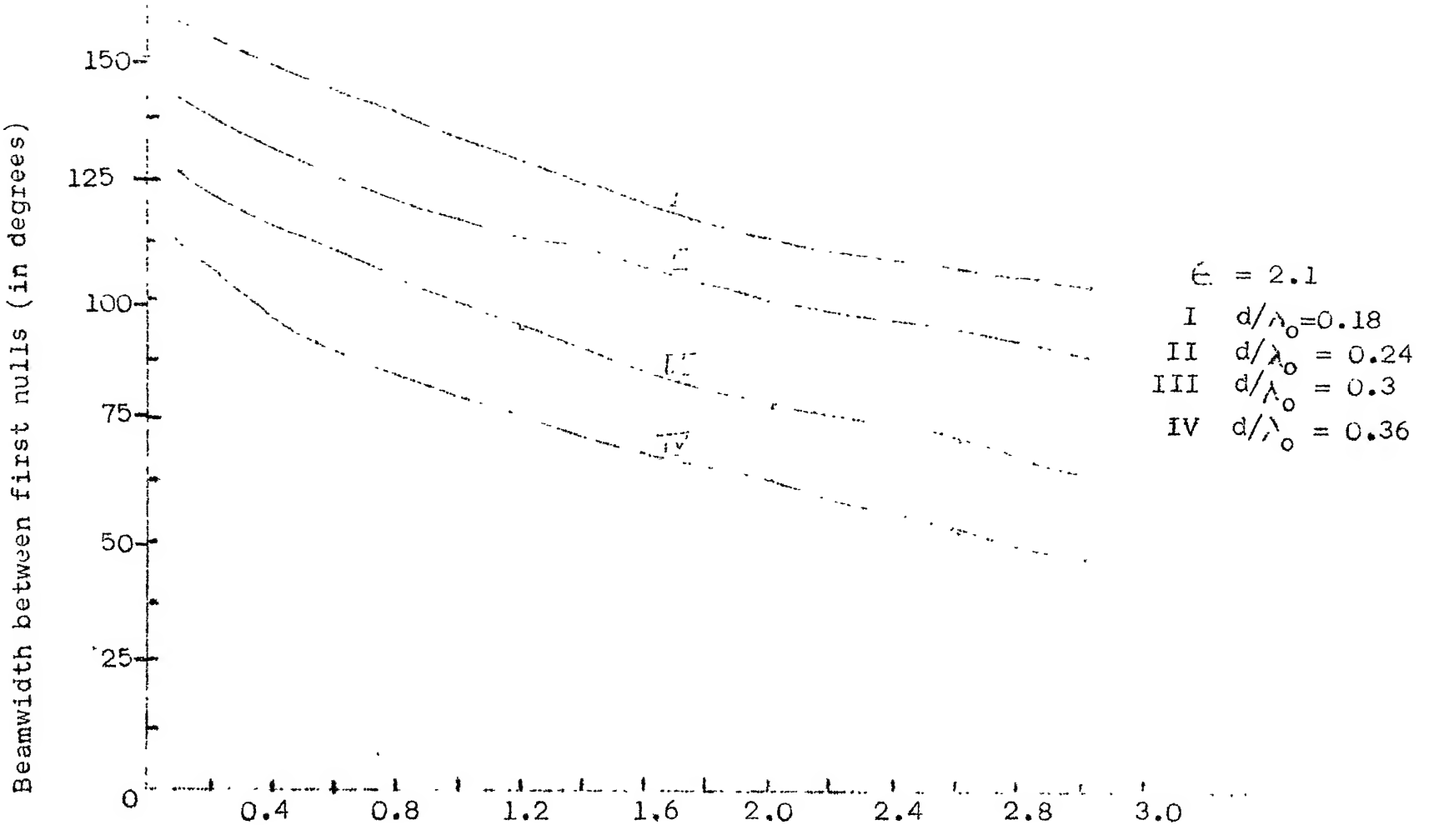

Fig. 4.8: Measured Dependence of beamwidth on L/λ_o

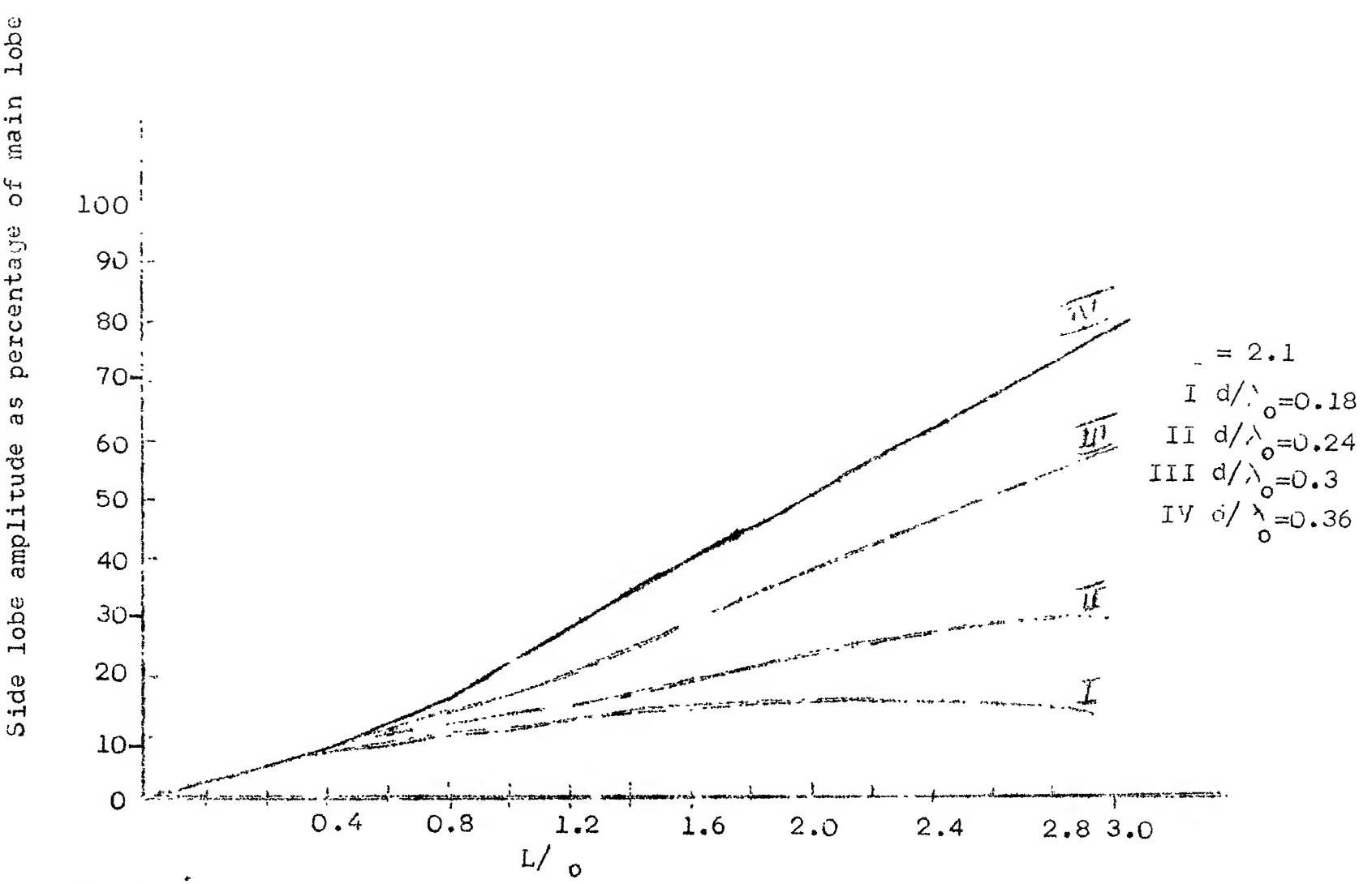

Fig. 4.9: Measured dependence of side lobes amplitude on L/ o

CHAPTER 5

CONCLUSIONS

With an objective to realise super-miniaturised antenna suitable for mobile communication systems, surveillance units and satellite communication systems it was intitutively anticipated that some specific type of dielectric materials may be effective to be used as receiving or transmitting antennas at lower frequency range. It is well known that because of associated short wave length, small sized antennas are many in number in millimeter and microwave frequency band with high directivity. Conveniently small sized antennas are available even at UHF/VHF range but the state of art as related to efficient antenna system at LF and ELF range is in very pessimistic form.

Dielectric antennas in general had been investigated extensively during forties and fifties. In order to understand with first hand experience, the radiating properties of dielectric rod antenna, we had selected low ϵ' Teflon to be used as receiving antenna at the scaled up microwave frequency band. To start with it was found that the Teflon antenna was simulated at some discrete microwave frequencies but lot of difficulties were faced to get reliable and steady results due to generator output instability and irregular behaviour of the test equipments/instruments.

In order to solve this problem an automated radiation plotter had been designed and constructed. Dielectric rod antennas of Teflon material of different diameter and lengths with different methods of excitation had been studied at some discrete microwave frequencies. The automated radiation plots which were verified for their short and long term repeatability have been included in the working chapter. For some specific diamentions and frequencies, excess radiation of the order of 7 dB have been recorded.

After some quantitative analysis of these results suitable material can be substituted for simulation of this antenna at the scaled down frequency band. And that will be beginning of break through of this dark region in the antenna field.

REFERENCES

1. D. HONDROS and P. DEBYE: Ann. Phys. LPZ., 32, 465 (1910).
2. H. ZAHN: Ann. Phys. LPZ, 49, 907 (1916).
3. O. SCHRIEVER: Ann. Phys. LPZ, 64, 645 (1920).
4. W.L. BARROW: Proceedings of IRE 24, 1298 (1936).
5. G.C. SOUTHWORTH: Bell System of Technical Journal, 15, 284(1936).
6. J.R. CARSON, S.P. MEAD, and S.A. SCHELKUNOFF: Bell System of Technical Journal 15, 310(1936).
7. P. MALLACH: Notes from unpublished german documents, Central Radio Bureau Library London.
8. H.J. WEGENER: Thesis for degree of Dr. Ing. Technical High School, Berlin (1944).
9. G.C. SOUTHWORTH: US Patent 2,206,923 (1941).
10. G.E. MUELLER and W.A. TYRRELL: Bell System of Technical Journal, 26, 837 (1947).
11. D.F. HALLIDAY and D.G. KIELY: Journal IEE 94, Pt. III A, 610 (1947).
12. R.B. WATSON and C.W. HORTON: Journal of Applied Physics 19, 836 (1948).
13. I. SIMON L'Onde Elect, 28, 278 (1948).
14. G. WILKIES: Proceedings of IRE 36, 206 (1948).
15. C.W. HORTON, F.C. KAKAL, Jr. and C.M. MCKINNEY: Journal of Applied Physics 21, 1279 (1950).
16. R.B. WATSON: Journal of Applied Physics, 22, 154 (1951).
17. R.B. ADLER: Proceedings of IRE vol. 40, pp. 339-348, March 1952.

18. J.O. SPECTOR and J. BROWN, Proceedings of IEE on Antenna and Propagation, vol. 1041B, pp. 27-34, Jan. 1957.

19. J.W. DUNCAN and R.H. DUHAMEL, Proceedings of IEE on Antenna and Propagation, pp. 284, Jul. 1957.

20. C.M. ANGULU and W.S.C. CHANG, Proceedings of IEE on Antenna and Propagation, pp. 207, Jul. 1959.

21. Proceedings of IEEE on Antenna and Propagation, pp. 506, July,1962.

22. Proceedings of IEEE on Antenna and Propagation, pp. 821, Sept. 1965.

23. Proceedings of IEEE on Antenna and Propagation, pp. 239, March,1966.

24. J.R. JAMES, Proceedings of IEEE on Antenna and Propagation, pp. 309, March 1967.

25. Proceedings of IEEE on Antenna and Propagation, pp. 122, March 1972.

26. Proceedings of IEEE on Microwave Theory and Technology, vol. MTT-18, pp. 1033, 1973.

27. Electronic Letter, vol. 9, pp. 148, 1973.

28. Proceedings of IEEE on Antenna and Propagation, pp. 577, July,1975.